Agtrap activity under both physiological and pathological conditions. The balance of the endogenous expression of Agtrap and AT1R in local tissues is important for the regulation of tissue AT1R signaling. Down-regulation of Agtrap and/or up-regulation of AT1R at local tissue sites together with the resultant pathological activation of the tissue renin-angiotensin system are pathogenetic mechanisms that may be responsible for cardiovascular and renal disease. For example, in Ang II-infused mice and genetically hypertensive rats, the development of hypertension and organ injury, such as cardiac hypertrophy and renal fibrosis, was reportedly accompanied by a decrease in the tissue Agtrap expression without altered AT1R expression (2, 15–19). In addition, we previously showed that serum starvation stimulates *Agtrap* gene expression in mouse distal convoluted tubule cells (mDCT cells) and that Runx3, one of the Runt-related transcription factors, is involved in the transcriptional activation of *Agtrap* gene expression (20). However, the regulatory mechanism of *Agtrap* gene expression in relation to organ injury needs further investigation to elucidate the relationship of the regulation of Agtrap expression with the pathophysiology of cardiovascular and renal disease at the molecular level.

The transcription factors upstream stimulatory factor (USF/Usf) 1 and USF2/Usf2 were originally identified in HeLa cells by biochemical analysis (21, 22). The human cDNA cloning of Usf1 and Usf2 revealed that the Usfs belong to the c-Myc-related family of DNA-binding proteins, which have a helix-loop-helix motif and a leucine repeat, and that USF interacts with its target DNA as a dimer (23). Previous examination of the tissue and cell type distribution of Usf1 and Usf2 revealed that although both are ubiquitously expressed, different ratios of USF homo- and heterodimers are found in different tissues and cell types (24). The results of mouse Usf1 cDNA cloning showed a high level of sequence homology between the mouse and human USF1 genes (25). Previous studies that were undertaken to assign a physiological role to the Usfs *in vivo*, including the disruption of Usf1 and Usf2 genes in mice, revealed that Usf1 and Usf2 play a role in the modulation of glucose and lipid metabolism by modulation of their trans-activating efficiency (26–29). Subsequent studies also showed that Usf1 and Usf2 are involved in the pathophysiology of several metabolic disorders, including familial hypercholesterolemia and diabetic nephropathy (30–33). In this study, we show that the proximal promoter region (−72 to −43) of the mouse *Agtrap* gene contains an "E-box (CANNTG)" sequence, which is a putative binding site for Usf1 and Usf2 that interacts with these transcription factors. It is shown both *in vitro* and *in vivo* that Usf1 decreases and Usf2 increases the *Agtrap* gene expression through their binding to the E-box.

EXPERIMENTAL PROCEDURES

Cell Culture—The mDCT cells were kindly provided by Dr. Peter A. Friedman (University of Pittsburgh School of Medicine). These cells have been shown to have a phenotype of a polarized tight junction epithelium along with both morphological and functional features retained from the parental cells (14, 34–36). The mDCT cells also express the endogenous AT1R and Agtrap (14). Human embryonic kidney-derived 293 (HEK293) cells were cultured according to the American Type Culture Collection (ATCC) protocol, as described previously (37, 38).

Animals and Treatment—Adult C57BL/6 mice were purchased from Oriental Yeast Kogyo (Tokyo, Japan). The procedure of unilateral ureteral obstruction (UUO) was performed using C57BL/6 mice, as described previously (20, 39). Briefly, with the mice under anesthesia, the left ureter was ligated with 4-0 silk at two locations and then cut between the ligatures to prevent retrograde urinary tract infection. Mice that were operated on were sacrificed under anesthesia 7 days after UUO. Sham operation was also performed in which the ureters were manipulated but not ligated. Seven days after the sham operation, mice were sacrificed to obtain control kidneys. The procedures were performed in accordance with the National Institutes of Health guidelines for the use of experimental animals. All of the animal studies were reviewed and approved by the Animal Studies Committee of Yokohama City University.

Plasmid Construction and Transcriptional Mouse Agtrap and Human AGTRAP Promoter Assay—For the analysis of the mouse *Agtrap* promoter, 5022-, 2943-, 2090-, 1272-, 972-, 613-, 453-, 374-, and 222-bp mouse Agtrap promoter fragments (−4950, −2871, −2018, −1200, −900, −541, −381, −302, and −150 to +72 of the putative transcriptional start site, respectively) were amplified from C57BL/6J genomic DNA, using the pair of primers indicated in Table 1, and then subcloned into the multicloning sites of pBluescript. A 613-bp *Agtrap* promoter fragment (−541 to +72 of the putative transcriptional start site)-containing plasmid was used as a template to construct mutations in the X-box, E-box, and GC-box by oligonucleotide (ODN)-directed mutagenesis (40–42). The sequences of the oligonucleotide used to create the mutated X-box (X-box mt), mutated E-box (E-box mt), mutated GC-box (GC-box mt, and mutated X- and E-boxes (X/E-box mt) are also shown in Table 1. To normalize transfection efficiency, we employed the Dual-Luciferase Assay System (Promega) for the transcriptional *Agtrap* promoter assay using pGL3-basic plasmid-based luciferase constructs, as described previously (20, 36).

For analysis of the human *AGTRAP* promoter, 575-bp *AGTRAP* promoter fragments (−480 to +95 of the putative transcriptional start site, NC_000001.9) containing two adjacent wild-type or mutated E-box motifs, were gene-synthesized (Eurofins MWG Operon). The human *AGTRAP* promoter assay using the Dual-Luciferase Assay System (Promega) was performed using pGL3- and pGL4.1-basic plasmid-based luciferase constructs (20, 36).

Real Time Quantitative RT-PCR Analysis—Total RNA was extracted and purified using the RNeasy kit (Qiagen), and the cDNA was synthesized using SuperScript VILO (Invitrogen). Real time quantitative RT-PCR was performed by incubating the RT product with the TaqMan Universal PCR Master Mix and designed TaqMan FAM™ dye-labeled probes for Usf1, Usf2, and Agtrap (Applied Biosystems), and a TaqMan VIC dye-labeled probe as the internal control (18 S rRNA Endogenous Control, Applied Biosystems) in the same reaction mixture (CFX96 system, BIO-RAD), essentially as described previously (20).

Immunoblot Analysis—A 14-amino acid synthetic peptide corresponding to amino acids 148–161 of the C-terminal tail of mouse (DBA/2J) ATRAP was used for the generation of a polyclonal anti-ATRAP antibody (7), and the characterization and specificity of the anti-ATRAP antibody were described previously (9, 15, 43). Antibodies for USF1 (C-20 sc-229, Santa Cruz Biotechnology), USF2 (ab32616, Abcam), TATA-binding protein (ab818[1TBP18], Abcam), and α-tubulin (ab40742 Abcam) were also used. Immunoblot analysis was performed as described previously (9, 15, 43), and the images were analyzed using a FUJI LAS3000mini Image Analyzer (FUJI Film, Tokyo, Japan).

Electrophoretic Mobility Shift Assay (EMSA)—Nuclear extracts from mDCT cells (70–80% confluent, a 15-cm diameter dish) were prepared with a modification of the protocols of Dignam *et al.* (44) and Swick *et al.* (45). The final protein concentration was adjusted to 1 mg/ml. EMSA was performed essentially as described previously (46, 47). Briefly, single-stranded ODN sequences were biotin-labeled at 3′-ends by the manufacturer, annealed to each other, and used as the probe. The ODN sequences for the E-box and mutated E-box (E-box mt) are shown in Table 1. Nuclear extracts (2 μg) were incubated on ice in a 20-μl EMSA binding reaction mixture containing 10 mM Tris-HCl, pH 7.5, 50 mM NaCl, 1 mM EDTA, pH 8.0, 4% glycerol, 1 μg of BSA, and 1 μg of double-stranded poly(dI-dC) in the presence or absence of a specific double-stranded competitor DNA and biotin-labeled DNA probe. The incubation mixture was loaded onto a 5% polyacrylamide mini (7.5 × 9.0 cm) gel in 0.5× TBE and electrophoresed at 350 V for 25 min, followed by transfer of DNA from the gel onto nylon membranes (Hybond-N+, GE) by cross-linking the transferred DNA to the membrane and rinsing with the TN buffer (100 mM Tris-HCl, pH 7.5, 150 mM NaCl). After blocking the incubation with Blocking Reagent (FP1020, PerkinElmer Life Sciences), incubating with streptavidin-horseradish peroxidase (HRP) conjugate (NEL750, PerkinElmer Life Sciences), and washing (incubation) to remove unreacted excess reagent with PBST (0.05% Tween 20/PBS), the biotin-labeled DNA was visualized by chemiluminescence (Immobilon Western Detection Reagent, Millipore) and analyzed using an LAS3000mini Image Analyzer (FUJI Film, Japan).

Streptavidin-Biotin Complex Assay—Streptavidin-biotin complex assay was performed using 3′-biotin-labeled oligonucleotides corresponding to the *Agtrap* E-box and X-box (Table 1), essentially as described previously (28, 48, 49). The streptavidin that was immobilized on agarose CL-4B (85881, Sigma) was pretreated with TN buffer containing 1% BSA and incubated with 50 μg of nuclear extracts from mDCT cells on ice in a 200-μl EMSA binding buffer for 20 min. After five washing steps with EMSA binding buffer, the streptavidin-biotin-DNA complex was eluted with SDS buffer, and a one-fifth volume was used for immunoblot analysis.

Chromatin Immunoprecipitation (ChIP) Assay—ChIP assay was performed essentially according to the manufacturer's protocol (Active Motif) (50, 51). Briefly, mDCT or HEK293 cells were treated with formalin to cross-link the protein-DNA complexes, and glycine was added to stop the reaction. The cells were lysed with 300 μl of lysis buffer (50 mM Tris-HCl, pH 8.0, 10 mM EDTA, pH 8.0, 1% SDS, protease inhibitor mixture; P8340, Sigma), and the lysates were sonicated using the Bioruptor Sonication System (250 watts, 30 s on and 30 s off/30 cycle; Bioruptor UCD-250, COSMO BIO, Tokyo, Japan) to reduce the DNA fragments. Subsequently, the sonicated lysates were divided into three equal aliquots for immunoprecipitation with specific antibodies, immunoprecipitation with control IgG (rabbit anti-HA antibody; 561, MBL, Japan), and input reference. After immunoprecipitation with an anti-USF1 antibody (C-20 sc-229, Santa Cruz Biotechnology), anti-USF2 antibody (C-20 sc-862, Santa Cruz Biotechnology), anti-SREBP1 antibody (H-160 sc-8984, Santa Cruz Biotechnology), anti-BMAL1 antibody (ab3350, Abcam), or control IgG, DNA was purified from the antibody-bound and unbound input fractions. The anti-USF1 antibody and anti-USF2 antibody used in the ChIP assay were characterized in detail in a previous study (28). Enrichment of the mouse *Agtrap* promoter sequences in the respective bound fractions was estimated by quantitative PCR with the SsoFast EvaGreen system (Bio-Rad) using the primers shown in Table 1 to detect the 134-bp fragment (−65 to +69 of the transcriptional start site).

For the ChIP analysis of human *AGTRAP*, HEK293 cells were treated with formalin to cross-link the protein-DNA complexes, and then the cells were lysed with lysis buffer and sonicated to reduce the DNA fragments. After immunoprecipitation with an anti-USF1 antibody, anti-USF2 antibody, anti-SREBP1 antibody, anti-BMAL1 antibody or control IgG, DNA was purified from the antibody-bound and unbound input fractions. Enrichment of the *AGTRAP* promoter or exon3 sequences in the bound fractions was estimated by quantitative PCR using the primers in Table 1 to detect 161- or 102-bp fragments, respectively. The target proteins in the co-immunoprecipitates were also subjected to immunoblot analysis and were visualized by TrueBlot (Affymetrix).

Statistical Analysis—All the quantitative data are expressed as the means ± S.E. For comparisons between groups, Student's *t* test was employed. Differences were considered to be statistically significant at $p < 0.05$.

RESULTS

Determination of the Minimal Mouse Agtrap Promoter—To determine the minimal region required for basal activity of the core promoter of the *Agtrap* gene, the 5-kb promoter region upstream of its transcriptional start site was isolated. Then, we generated a series of luciferase reporter plasmids containing the various *Agtrap* proximal promoter regions, which are illustrated in Fig. 1*A*. To determinate the minimal *Agtrap* promoter, we transfected these plasmids into mDCT cells, and luciferase activity was measured. Although the luciferase activity was gradually increased by the deletion from −4950 to −541, further deletion, *i.e.* from −381 to −150, resulted in a decrease in the luciferase activity of the *Agtrap* reporter constructs (Fig. 1*A*). Consistent with this finding, this region contains two important *Agtrap* regulatory elements, the SMAD-binding element (−261 to −257) and the Runt-binding element (−246 to −241) (20). Intriguingly, the promoter region from −150 to +72 maintained the luciferase activity of the *Agtrap* reporter constructs. This suggested that this region contains important

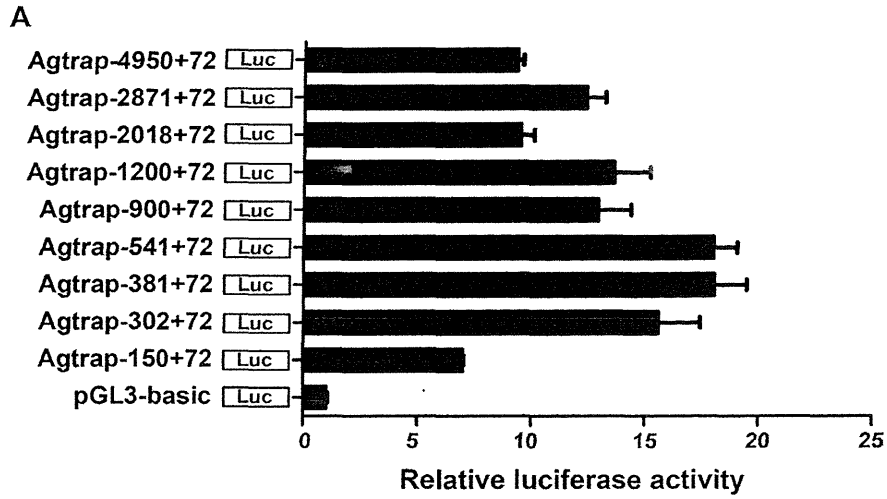

B

```
-555  TATACGAATG TCTCACCTGC CTGTGTGTGT ATATGCACTT GTGTCTGGAG

-505  CCTGCGGAGG ACAAAAGAGG GTGGTTGTAT CACAAGTACA TGATTGTGAG
                 STATx
-455  CCGGCATGTG GGTTCTGGGA ACCCAAGCCT AGAAAAAGTA GTAACATGTG
                                                 CdxA
-405  CTCTTAATCA CGGAATCCTC TCCAACCCTC ACTTTTTATC TTTATGGACA

-355  TGAATTCATT CACTGATCCT CACAAAGATG ATGAGGTAGG CACTGTTCTA
                 Ets1                Ets1              SBE
-305  ATTCTTGTGC AAGGGAAGTA AGAGAGGAGA GAGGATGTTC TGGGCAGACA
                 RBE                                    c-Myb
-255  CCAACTGTTA CCACACCCGC AGTTTCTGCC CGCTTGCCCC AGGCTCCTCT
-205  GGCTGTAGGT CGTCCCACCA CCTCACCTCG ATCCCACTTA GGCAGCCCGT

-155  TGAGCCCCTA GGCTGCAGAA ATCCCGACCT CCTGGCTTGA AGCACAGGAG

-105  CTGGTAGGAG GCCTAGGCAG TAGTAGTAGC AGGAGCCTGA GCCTAGCAGC
           AP-4              X-box                    E-box
 -55  AAGAGCACTG CCTGACGCCG TCTCCTAGCA ACCGGCTGCA GTCACGTGGC
                   v-Myb                          GC-box
  -5  CGCGCGAGTT GGCCTCCCGC CGTTGGAACT GGCGCAACGC GACGGGCGGG

 +46  GCCAGGAAGT TTGTTCCCGA GTTCGGAGCC CAGGAGTCCC CGCGGCCGTC

 +96  GCTCAGGTGC CCTCCGCCGG GTCGGGATGG AGCTGCCTGC CGTGAACTTG

+146  AAGgtggccg cgcggccggg cgggcggggg tccaggaacc tggggaacgg
```

FIGURE 1. **Identification of mouse *Agtrap* promoter region.** *A*, functional analysis of the mouse *Agtrap* promoter in mDCT cells. The *Agtrap* promoter-luciferase constructs were transiently transfected into mDCT cells, and luciferase assay was performed. The relative luciferase activities were calculated relative to those achieved with the promoterless control plasmid (pGL3-basic). Data are expressed as the means ± S.E. ($n = 4$). *B*, nucleotide sequence of the mouse *Agtrap* promoter region and putative transcription factor-binding motifs. The nucleotides are numbered at the *left* with the putative initiation site of transcription designated as +1. The untranslated and translated nucleotides of exon 1 are designated by the *bold letters* and the *bold italic letters*, respectively. The nucleotides in a portion of intron 1 are indicated by the *small letters*.

regulatory elements for *Agtrap* gene transcription. To identify the candidate transcription factors involved in *Agtrap* gene transcription, we next performed a computational sequence analysis of the *Agtrap* proximal promoter region using TFSEARCH: Searching Transcription Factor-binding Sites software and identified the consensus binding motifs for several transcription factors (Fig. 1*B*).

Functional Involvement of X-box, E-box, and GC-box in the Proximal Mouse Agtrap Promoter Activity—Among the consensus binding motifs of the transcription factors listed in Fig. 1*B*, there are highly homologous sequences of the X-box (5′-GTCCCTAGCAAC-3′) (52), E-box (5′-CATGTG-3′ or 5′-CANNTG-3′), and GC-box (5′-GGAGGGGGG(A/C)GG-3′) (53), which are highly conserved in mammals (Fig. 2*A*). To examine the functional role of these conserved elements in the regulation of *Agtrap* gene transcription, we mutated the core binding sequences of the X-box, E-box, and GC-box in the *Agtrap* promoter, X-box mt, E-box mt, and GC-box mt (Fig. 2*B*). Although the promoter region from −541 to +72 of the putative transcriptional start site of the *Agtrap* gene exhibited substantial luciferase activity in mDCT cells, site-directed mutations of the X-box, E-box, or GC-box decreased the luciferase activity to 39.7 ± 2.5% (X-box mt), 48.2 ± 4.1% (E-box mt), and 51.2 ± 3.0% (GC-box mt) of that achieved with the wild-type promoter, respectively (Fig. 2*C*). Mutations of any two of the three consensus motifs further decreased the lucif- F2

tapraid4/zbc-bc/zbc-bc/zbc02913/zbc5349-13z ZSUBMIT 17 xppws S=5 21/5/13 2:59 | 4/Color Figure(s) F3 | ARTNO: M113.451054

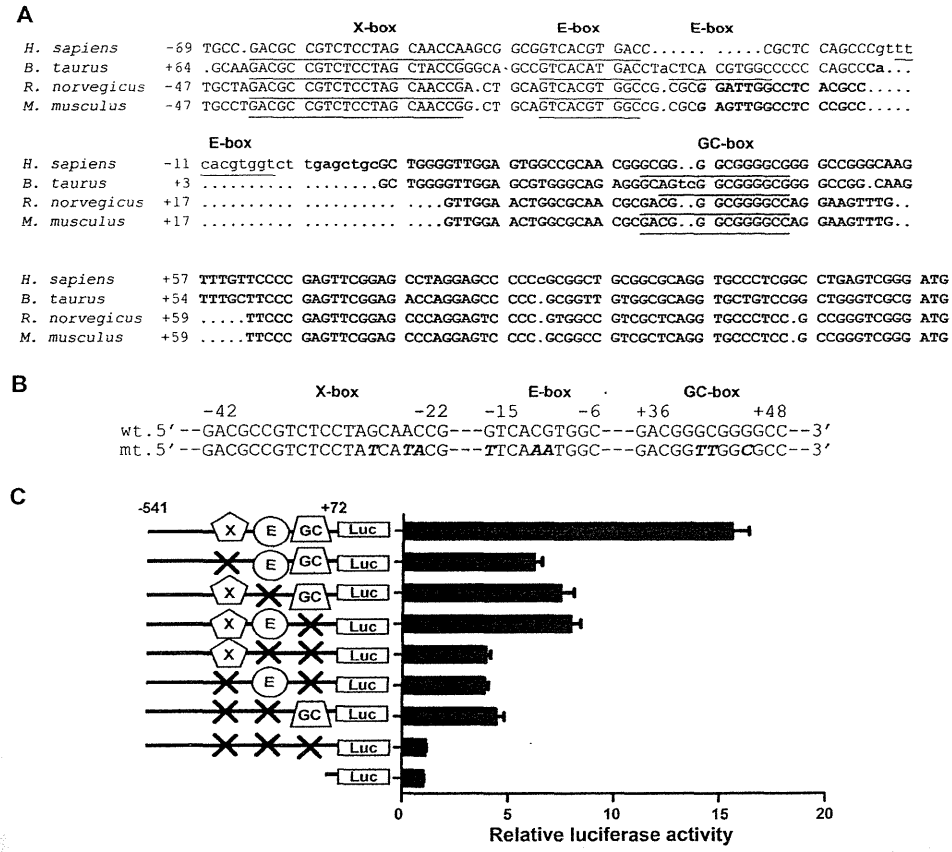

FIGURE 2. **Involvement of the X-box, E-box, and GC-box regions in the transcriptional activation of the mouse *Agtrap* promoter in mDCT cells.** *A*, alignment of the proximal regions of the human (*Homo sapiens*), cow (*Bos taurus*), rat (*Rattus norvegicus*), and mouse (*Mus musculus*) *Agtrap* genes. The nucleotides are numbered at the *left* with the putative initiation site of transcription designated as +1. The putative transcription factor binding motifs are indicated with *underlines*. *B*, construction of site-directed mutations in the X-box, E-box, and GC-box in the mouse *Agtrap* promoter sequence. Wild-type sequences (*wt*) and mutated sequences (*mt*) are shown. *C*, effects of mutations in the X-box, E-box, and GC-box on the transcriptional activity of the mouse *Agtrap* promoter (−541 to +72 of the transcriptional start site)-luciferase hybrid gene in mDCT cells. The relative luciferase activities were calculated relative to those achieved with the promoterless control plasmid. Data are expressed as the means ± S.E. ($n = 4$).

erase activity (E-box/GC-box mt, 25.3 ± 1.4%; X-box/GC-box mt, 24.7 ± 1.3%; X-box/E-box mt, 28.6 ± 2.4%) relative to that achieved with the wild-type promoter, whereas mutation of all three motifs reduced the luciferase activity almost to the background reference level (X-box/E-box/GC-box mt, 7.2 ± 0.3%). These results indicate that the three binding motifs of the X-box, E-box, and GC-box are important for the basal transcriptional activity directed by the minimal *Agtrap* promoter and suggest that these binding motifs independently modulate the promoter activity of the *Agtrap* gene.

Identification of the E-box as a Transcription Factor-binding Site in the Mouse Agtrap Promoter—Among the X-box, E-box, and GC-box in the *Agtrap* proximal promoter, the canonical E-box is a target for many genes involved in pathophysiological conditions such as diabetic nephropathy and fibrotic disease (33, 54, 55). Therefore, we focused on the functional characterization of the E-box in the regulation of the *Agtrap* promoter. To determine whether the E-box is capable of binding transcription factors, nuclear extracts were prepared from mDCT cells (Fig. 3*A*), and EMSA analysis was performed with an Agtrap promoter fragment (−72 to −43) probe containing the E-box but not the X-box or GC-box (Table 1). The E-box probe formed a DNA-protein complex (Fig. 3*B*, *lanes 8* and *12*), and the formation of the complex was completely impaired by the addition of an excess amount of the unlabeled probe with a wild-type sequence (Fig. 3*B*, *lanes 5–7*), but not by a mutated probe (Fig. 3*B*, *lanes 9–11*). These results indicate that there are nuclear factors that bind to the E-box sequence of the *Agtrap* promoter.

Specific Binding of Usf1 and Usf2 to the E-box of the Mouse Agtrap Promoter—Several candidate transcription factors, including Usf1, Usf2, BMAL1/Arntl, and Srebf1, are reported to be capable of binding to the E-box sequence. Among these factors, Usf1, Usf2, and BMAL1/Arntl, but not Srebf1 mRNA, were detectably expressed on RT-PCR and immunoblot analyses in mDCT cells (data not shown). We then examined whether Usf1, Usf2, and/or BMAL1 interact with the E-box of the *Agtrap* promoter using a biotin-labeled E-box probe and X-box probe. These biotin-labeled probes were individually mixed with the nuclear extracts of mDCT cells and pulled down using streptavidin-Sepharose. The results showed that substantial amounts of Usf1 (43 kDa) and Usf2 (44 kDa) proteins from nuclear extracts were pulled down with the biotin-labeled E-box, but not the X-box, of the *Agtrap* promoter (Fig. 4*A*). However, no binding of BMAL1 to the biotin-labeled E-box or X-box in the *Agtrap* promoter was observed.

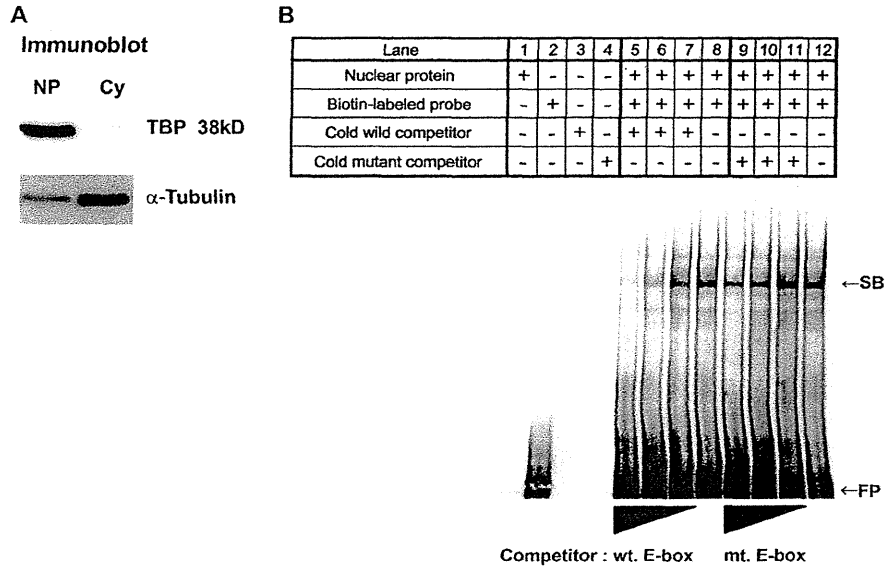

Q: A FIGURE 3. **Identification of nuclear factors binding to the E-box (−72 to −43) of the mouse *Agtrap* promoter by EMSA.** *A*, immunoblot analysis shows TATA-binding protein (*TBP*) and α-tubulin in the nuclear extract (*NP*) and cytosolic extract (*Cy*), respectively. *B*, electrophoretic mobility shift and competition analyses of complexes formed by nuclear factors with the E-box (−72 to −43) of the *Agtrap* promoter. The E-box ODNs were biotin-labeled at the 3′-end and used as the labeled probe. Nuclear extracts (2 μg) from mDCT cells were incubated with the probe. In electrophoretic shift competition assay, 50, 12.5, and 2.5 pmol of unlabeled wild-type E-box (*wt*) or mutated E-box (*mt*) ODNs were added to the reaction mixture. *SB* indicates a shifted band derived from specific DNA-protein complexes. *FP*, free probes.

We next performed ChIP analysis to determine whether Usf1 and Usf2 physiologically interacted with the *Agtrap* promoter region. As shown in Fig. 4*B*, the 134-bp E-box containing the sequence from −65 to +69 of the transcriptional start site of the *Agtrap* promoter was recovered from mDCT cells after immunoprecipitation of sheared genomic DNA with an anti-USF1 antibody and anti-USF2 antibody but not after immunoprecipitation with an anti-SREBP1 antibody or anti-BMAL1 antibody. Quantitative PCR analysis confirmed that Usf1 and Usf2 are present in the *Agtrap* E-box promoter region, and the corresponding genomic DNA was enriched with both an anti-USF1 antibody (*, $p < 0.05$, *versus* IgG control) and anti-USF2 antibody (**, $p < 0.01$, *versus* IgG control) but not with an anti-SREBP1 antibody or anti-BMAL1 antibody. These data provide evidence for the occupancy by Usf1 and Usf2, but not Srebf1 or BMAL1, of the mouse *Agtrap* promoter E-box *in vivo*.

Functional Involvement of Usf1 and Usf2 in Mouse Agtrap Promoter Activity—To determine whether Usf1 and Usf2 are involved in the transcriptional regulation of the *Agtrap* gene in mDCT cells, we examined the effect of Usf1 and Usf2 siRNAs transfection on endogenous Agtrap gene expression. The mRNA and protein levels of Usf1 (Fig. 5, *A* and *D*) and Usf2 (Fig. 5, *B* and *E*) were significantly decreased after transfection with their respective siRNA. In addition, although the Usf2 mRNA level was slightly increased by Usf1 knockdown (Fig. 5*B*), the Usf2 protein level was not affected (Fig. 5*E*). Intriguingly, although the siRNA reduction of Usf1 resulted in a significant increase in the levels of the Agtrap mRNA (Fig. 5*C*, $p < 0.01$, siUsf1 *versus* siCtrl) and protein (Fig. 5*F*, $p < 0.01$, siUsf1 *versus* siCtrl), Usf2 knockdown significantly decreased the Agtrap mRNA (Fig. 5*C*, $p < 0.01$, siUsf2 *versus* siCtrl) and protein (Fig. 5*F*, $p < 0.01$, siUsf1 *versus* siCtrl). These results show that Usf1 and Usf2 exert negative and positive regulatory effects on Agtrap gene expression, respectively.

Pathophysiological Relevance of Usf1 and Usf2 in Mouse Agtrap Gene Expression in the Kidney—To understand the pathophysiological roles of Agtrap in target organ injury, it is necessary to investigate the regulation of the expression of the *Agtrap* gene in response to pathological stimuli. UUO is a well established experimental model of progressive tubulo-interstitial fibrosis. UUO leads to changes in renal hemodynamics, inflammatory responses in the kidney, tubular hypertrophy, and interstitial fibrosis of the affected kidney by stimulating the renin-angiotensin system (39). Since we previously showed that the Agtrap mRNA level was suppressed in the affected kidney by UUO (20), we examined whether the change in *Agtrap* gene expression is accompanied by any modulation of the *Usf1* or *Usf2* gene expression in the UUO kidney. According to the results of quantitative RT-PCR analysis, while the Usf1 mRNA expression was significantly up-regulated in the affected kidney after 7 days of UUO (Fig. 6*B*), the Usf2 mRNA expression was significantly down-regulated in the affected kidney by UUO (Fig. 6*C*), with a concomitant decrease in the Agtrap mRNA expression (Fig. 6*A*). These results *in vivo* are consistent with the notion that Usf1 and Usf2 are inhibitory and stimulatory transcription factors for the *Agtrap* gene, respectively.

Functional Involvement of the Two Adjacently Located E-box Motifs in Proximal Human AGTRAP Promoter Activity—To evaluate the evolutionary and functional conservation of the regulation of *AGTRAP* gene expression by the E-box, we examined the activity of the *AGTRAP* proximal promoter with or without an E-box mutation using luciferase reporter assay. Because the promoter of the human isologous gene *AGTRAP* has two adjacently located E-box motifs (Fig. 2*A*), we analyzed both of them. As shown in Fig. 7*A*, the 575-bp human *AGTRAP* proximal promoter fragments (−480 to +95 of the putative transcriptional start site) exhibited substantial luciferase activity in human kidney-derived HEK293 cells. In addition, muta-

TABLE 1
Primer sequences used in the study

Primers		Primer sequences
Construction of wild-type and mutated *Agtrap* promoter-containing plasmids		
−4950 to −353	Forward	5′GCCATTCCCTGAGCTGTTGAGGGCCCTTCACTGAAAGGCTTCTTGGT3′
	Reverse	5′CTTTGTGAGGATCAGTGAATGAATTCATGTCCATAAAGATAAAAAGTGA3′
−2871 to 353	Forward	5′CTAGAGAAGGTACCCAAGGAGCTAAACGGATCTGCAACCCTATAG3′
	Reverse	5′CTTTGTGAGGATCAGTGAATGAATTCATGTCCATAAAGATAAAAAGTGA3′
−2018 to −353	Forward	5′GCTATGTGGTTAAAGGCACTTGCCACACCAGCCTGTCGACTGGCC3′
	Reverse	5′CTTTGTGAGGATCAGTGAATGAATTCATGTCCATAAAGATAAAAAGTGA3′
−1200 to +72	Forward	5′ggggtaCCAACTTTTGCTATGTTGGGCAAGTGGACTCCA3′
	Reverse	5′cgggatccGAACTCGGGAACAAACTTCCT3′
−900 to +72	Forward	5′ggggtaCCCCTTTCTTGACTTCAGGTCCTGTCTCCCTTTCC3′
	Reverse	5′cgggatccGAACTCGGGAACAAACTTCCT3′
−541 to +72	Forward	5′gcggtACCTGCCTGTGTGTGTATATGCACTT3′
	Reverse	5′cgggatccGAACTCGGGAACAAACTTCCT3′
−381 to +72	Forward	5′gcggtACCCTCACTTTTTATCTTTATGG3′
	Reverse	5′cgggatccGAACTCGGGAACAAACTTCCT3′
−302 to +72	Forward	5′ggggtacCTTGTGCAAGGGAAGTAAGA3′
	Reverse	5′cgggatccGAACTCGGGAACAAACTTCCT3′
−150 to +72	Forward	5′gcggtaCCCTAGGCTGCAGAAATCCC3′
	Reverse	5′cgggatccGAACTCGGGAACAAACTTCCT3′
Construction of mutated *Agtrap* promoter-containing plasmids		
X-box-mt	Forward	5′CTGCCTGACGCCGTCTCCTATCATACGGCTGCAGTCACGTGGCCG3′
	Reverse	5′CGGCCACGTGACTGCAGCCGTATGATAGGAGACGGCGTCAGGCA3′
E-box-mt	Forward	5′TCCTAGCAACCGGCTGCATTCAAATGGCCGCGCGAGTTGGCCT3′
	Reverse	5′AGGCCAACTCGCGCGGCCATTTGAATGCAGCCGGTTGCTAGGA3′
GC-box-mt	Forward	5′GAACTGGCGCAACGCGACGGTTGGCGCCAGGAAGTTTGTTCCCGA3′
	Reverse	5′TCGGGAACAAACTTCCTGGCGCCAACCGTCGCGTTGCGCCAGTTC3′
X/E-box-mt	Forward	5′TCCTATCATACGGCTGCATTCAAATGGCCGCGCGAGTTGGCCT3′
	Reverse	5′AGGCCAACTCGCGCGGCCATTTGAATGCAGCCGTATGATAGGA3′
Electrophoretic mobility shift assay (EMSA) and oligonucleotide precipitation assay		
E-box ODN		5′CCGGCTGCAGTCACGTGGCCGCGCGAGTTG3′ and 5′CAACTCGCGCGGCCACGTGACTGCAGCCGG3′
E-box-mt ODN		5′CCGGCTGCATTCAAATGGCCGCGCGAGTTG3′ and 5′CAACTCGCGCGGCCATTTGAATGCAGCCGG3′
X-box ODN		5′CTGCCTGACGCCGTCTCCTAGCAACCGGCTG3′ and 5′CAGCCGGTTGCTAGGAGACGGCGTCAGGCAG3′
Chromatin immunoprecipitation (ChIP) assay		
Mouse *Agtrap* promoter	Forward	5′CCTAGCAGCAAGAGCAGCT3′
	Reverse	5′GAACTCGGGAACAAACTTCCT3′
Human *AGTRAP* promoter	Forward	5′ACAGTCCGCTTCCTGGAATA3′
	Reverse	5′GCCGCTTGGTTGCTAGGAGACGGCGTCGGCAGC3′
Human *AGTRAP* exon 3	Forward	5′GGCTGCATTGTATTCTCAGG3′
	Reverse	5′CTTATGGCGTCGATGGAGTC3′

tions of either of the two adjacently located E-box motifs significantly decreased the luciferase activity (Fig. 7*A*). Mutations of both E-box motifs further reduced the luciferase activity (Fig. 7*A*). These results indicate that the two adjacently located E-box motifs are important for the basal transcriptional activity directed by the *AGTRAP* promoter.

USF1 and USF2 Bind the AGTRAP Promoter Region—We further performed ChIP analysis to examine whether USF1, USF2, or BMAL1 physiologically interacts with the *AGTRAP* promoter region. For ChIP analysis, we prepared primer sets for the *AGTRAP* promoter region and internal exon 3 (Fig. 7*B*). A 161-bp fragment of the proximal upstream region of the two adjacently located E-box motifs in the *AGTRAP* promoter was recovered after immunoprecipitation of sheared genomic DNA from HEK293 cells with an anti-USF1 antibody and anti-USF2 antibody but not after immunoprecipitation with an anti-SREBP1 antibody or anti-BMAL1 antibody. Quantitative PCR analysis showed that USF1 and USF2 are present at the *AGTRAP* E-box promoter region, and the corresponding genomic DNA was enriched with an anti-USF1 antibody (**, $p < 0.01$, *versus* IgG control) and anti-USF2 antibody (**, $p < 0.01$, *versus* IgG control), respectively, but not with an anti-SREBP1 antibody or anti-BMAL1 antibody (Fig. 7*B*). Among these factors USF1 and USF2, but not BMAL1 and SREBP1, proteins were also detected in the co-immunoprecipitates from HEK293 cells on immunoblot analyses (Fig. 7*C*). However, USF1, USF2, SREBP1, and BMAL1 did not interact with the *AGTRAP* exon 3 region, which is a negative control region, without the E-box (Fig. 7*B*). These data indicate the occupancy by USF1 and USF2, but not SREBP1 or BMAL1, of the human *AGTRAP* promoter region.

DISCUSSION

Despite the accumulating evidence supporting the involvement of an altered expression of *Agtrap* gene at local tissue sites in the pathogenesis of hypertension and related kidney injury, little is known about the transcriptional regulation of *Agtrap* expression. In this study, we showed that the promoter region from −150 to +72 of the mouse *Agtrap* 5′-flanking sequence, which is considered to contain important regulatory elements, directs *Agtrap* gene transcription in normal culture.

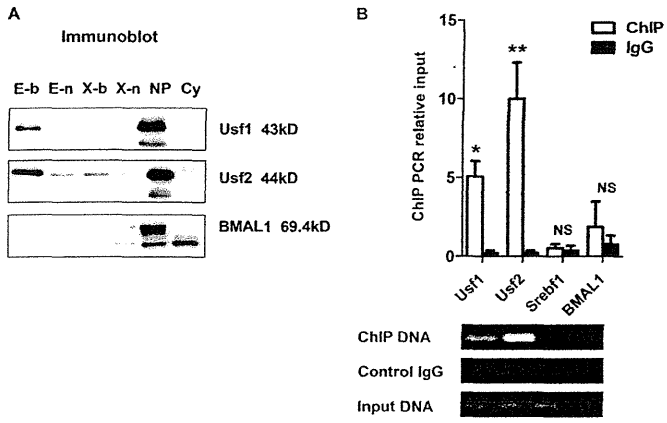

FIGURE 4. **Identification of Usf1 and Usf2 interaction with the E-box (−72 to −43) of the mouse *Agtrap* promoter by streptavidin-biotin complex assay and ChIP assay.** *A*, streptavidin-biotin complex assay. Nuclear extracts from mDCT cells were incubated with streptavidin immobilized on agarose beads. The streptavidin-biotin-DNA complex was eluted with SDS buffer and visualized by immunoblot analysis. *E-b*, E-box biotin-labeled probe; *E-n*, E-box nonlabeled probe; *X-b*, X-box biotin-labeled probe; *X-n*, X-box nonlabeled probe; *NP*, nuclear extracts; *Cy*, cytosolic extracts. *B*, ChIP assay. The mDCT cells were treated with an anti-USF1 antibody, anti-USF2 antibody, anti-SREBP1 antibody, anti-BMAL1 antibody, or control IgG (rabbit anti-HA antibody). Co-immunoprecipitated DNA was purified and estimated by quantitative PCR. In the *upper panel* the relative amount of DNA fragment detected per antibody is shown. In the *lower panel*, the quantitative PCR products, which were loaded on 3% agarose gels and visualized by ethidium bromide staining, are shown. Experiments were independently repeated at least three times, and data are expressed as the means ± S.E. *, $p < 0.05$; **, $p < 0.01$, *versus* control IgG. *NS*, not significant.

We analyzed the region from −381 to +72 based on the results showing maximum promoter activity. The results of luciferase assay using deletion mutants revealed the minimally required proximal promoter region from −150 to +72 that contains the X-box, E-box, and GC-box consensus motifs is able to direct substantial transcription of the *Agtrap* gene. Among these binding motifs, we confirmed that the E-box specifically binds Usf1 and Usf2 by employing EMSA, streptavidin-biotin complex assay, and ChIP. Such E-box-Usf1/Usf2 binding is functionally important in activating *Agtrap* expression for the following reasons: 1) mutation of the E-box to prevent Usf1/Usf2 binding reduces *Agtrap* promoter activity (Fig. 2); 2) transfection of siRNA for Usf1 increases and Usf2 decreases endogenous Agtrap mRNA and protein expression (Fig. 5), and 3) the decrease in Agtrap mRNA expression in the affected UUO kidney is accompanied by changes in Usf1 and Usf2 mRNA (Fig. 6). Taken together, these data indicate that Usf1 and Usf2 negatively and positively regulate *Agtrap* gene transcription, respectively. Because Usf1 and Usf2 bind to DNA with the same E-box sequence specificity, they most likely regulate *Agtrap* gene expression in a competitive manner.

Recently, the E-boxes in the promoter regions of renin and angiotensinogen were shown to be direct targets of Usf1 and Usf2 and suggested to be involved in the pathogenesis of both hypertension and renal injury (33, 56–58). In this study, it is

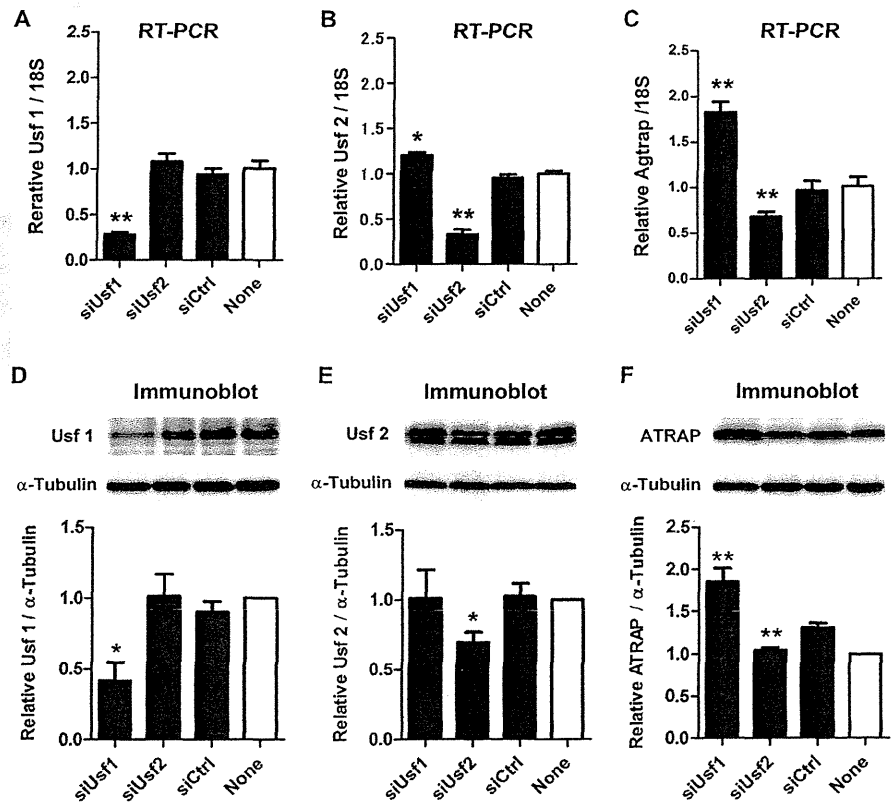

FIGURE 5. **Effects of specific knockdown of Usf1 and Usf2 by small interference (si)RNA on endogenous *Agtrap* gene expression in mDCT cells.** *A–C*, quantitative RT-PCR analysis showing the effects of respective siRNA transfection on the relative Usf1 (*A*), Usf2 (*B*), and Agtrap (*C*) mRNA levels. RNA quantity was normalized to the signal generated by constitutively expressed 18 S rRNA and is expressed relative to that achieved with extracts derived from nontreated mDCT cells (none). Experiments were independently repeated at least three times, and the data are expressed as the means ± S.E. *, $p < 0.05$; **, $p < 0.01$, *versus* control siCtrl. *D–F*, immunoblot analysis showing the effects of the respective siRNA transfection on the relative Usf1 (*D*), Usf2 (*E*), and Agtrap (*F*) protein levels. Representative immunoblots are shown, and protein expression levels are expressed relative to those achieved with extracts derived from nontreated mDCT cells (*none*). Experiments were independently repeated at least three times, and data are expressed as the means ± S.E. *, $p < 0.05$; **, $p < 0.01$, *versus* control siCtrl.

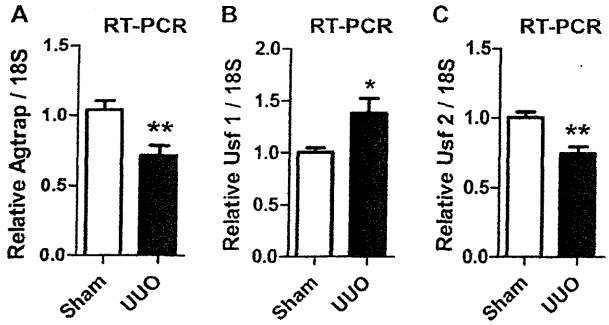

FIGURE 6. **Regulation of Usf1, Usf2, and *Agtrap* mRNA in the affected kidney by UUO.** *A–C*, quantitative RT-PCR analysis showing the effects of UUO on the relative Agtrap (*A*), Usf1 (*B*), and Usf2 (*C*) mRNA levels. RNA quantity was normalized to the signal generated by the constitutively expressed 18 S rRNA and is expressed relative to the level achieved with extracts derived from sham-operated kidney ($n = 6$). *, $p < 0.05$; **, $p < 0.01$, *versus* sham. Data are expressed as the means ± S.E.

shown that Agtrap, an emerging modulator of the renin-angiotensin system, is another target gene of Usf1 and Usf2, and that *Agtrap* gene expression is activated through the binding of Usf2 and inhibited through the binding of Usf1 to the same canonical E-box sequence in the *Agtrap* proximal promoter region.

Both Usf1 and Usf2 are reportedly activators of gene transcription via homodimerization or heterodimerization, with similar trans-activating capacities (59, 60), and they have also been proposed to function as repressors of a number of target genes (61). However, the results of this study show that Usf1 and Usf2 exert opposing regulatory effects on the expression of the same gene. Consistent with this notion, similarly opposing effects of Usf1 and Usf2 on the E-box of plasminogen activator inhibitor-1 gene, a key regulator of the fibrinolytic system, have been reported (62, 63). With respect to an interaction between Usf and other transcription factors, a previous study reported a contrasting functional and physical interaction between Usf and Sp1, a GC-box binding transcription factor, in the transcriptional regulation of the deoxycytidine kinase gene in liver-derived HepG2 cells (64). In the regulation of the deoxycytidine kinase promoter, the combination of Usf1 and Sp1 exhibited additive trans-activation at lower concentrations of Sp1, although Sp1 was inhibitory at higher levels, whereas trans-activation by Usf2 and Sp1 was synergistic in HepG2 cells (64). In this study, although the E-box and GC-box were found to be adjacently located in the *Agtrap* promoter, the results of luciferase assay showed a positive and independent stimulatory effect of these binding motifs in kidney-derived mDCT cells (Fig. 2), possibly because of a difference in the network of transcription factors in the liver and kidney. However, it is still possible that a functional interplay of Usf1 and Usf2 with putative transcription factors other than Sp1 is involved in the opposing regulatory effect exerted by Usf1 and Usf2 on *Agtrap* gene expression (Fig. 5). Further studies are needed to elucidate the molecular mechanisms, including kinase cascades, such as PI3K (28), which are involved in the differential regulatory functional effect of Usf1 and Usf2 on *Agtrap* gene expression. Studies are also needed to examine the possible role of E-box modulation by methylation at the core CpG in the Usf1/Usf2 recognition site (5′-CACpGTG-3′) in the regulation of the *Agtrap* promoter (64).

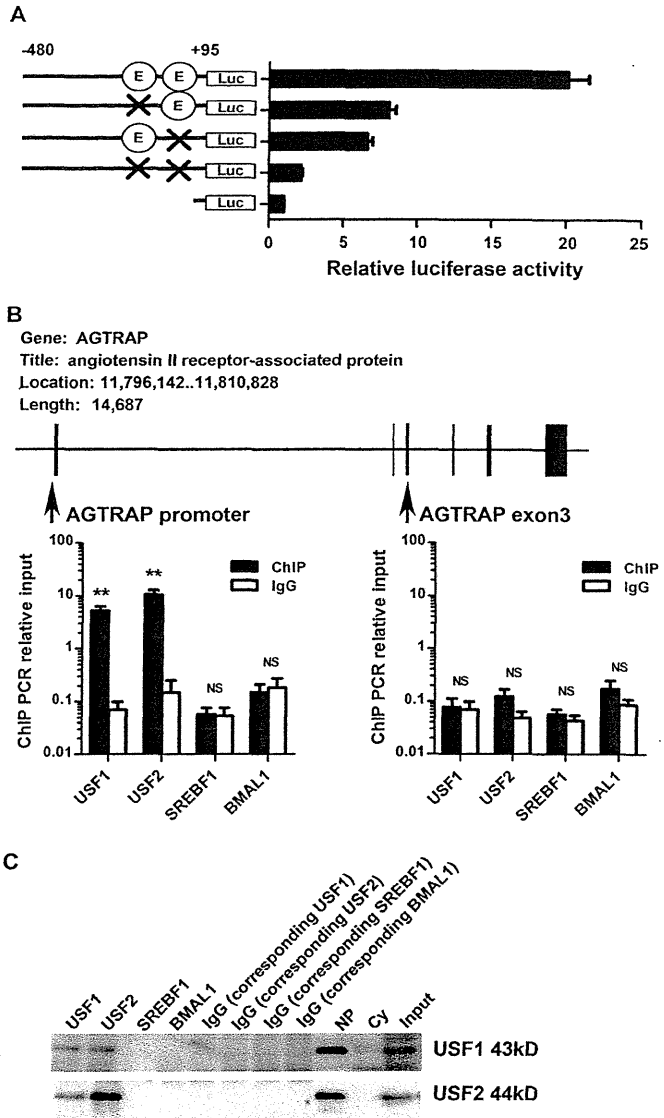

FIGURE 7. **Involvement of the E-box motifs in the regulation of the human *AGTRAP* promoter.** *A*, involvement of the two E-box motifs in the transcriptional activation of the *AGTRAP* promoter in HEK293 cells. The effects of mutations in the two E-box motifs on the transcriptional activity of the *AGTRAP* promoter-luciferase hybrid gene in HEK293 cells are shown. The relative luciferase activities were calculated relative to those achieved with the promoterless control plasmid. Data are expressed as the means ± S.E. ($n = 4$). *B*, identification of USF1 and USF2 interaction with the *AGTRAP* proximal promoter region by ChIP analysis. Schematic representation of the *AGTRAP* gene structure and the approximate genomic positions for the enrichment of the *AGTRAP* promoter and exon3 region by ChIP assay are shown (*upper panel*). The results of ChIP assay with an anti-USF1 antibody, anti-USF2 antibody, anti-SREBP1 antibody, or anti-BMAL1 antibody are shown (*lower panel*). Data are expressed as the means ± S.E. ($n = 4$). **, $p < 0.01$, *versus* control IgG (rabbit anti-HA antibody). *NS*, not significant. *C*, identification of USF1 and USF2 in the co-immunoprecipitates from the AGTRAP proximal promoter region in ChIP analysis. Co-immunoprecipitated proteins with respective specific antibodies or their corresponding control IgG in ChIP assay were subjected to immunoblot analysis and were visualized by TrueBlot (Affymetrix). *NP*, nuclear extracts; *Cy*, cytosolic extracts; *Input*, input reference.

Cardiovascular and renal diseases are closely related to circadian rhythms, which are under the control of an internal biological clock mechanism. The binding of the transcription factors BMAL1 and CLOCK to multiple extra- and intragenic E-boxes is reported to play an important role in the circadian

rhythm-related regulation of certain genes in peripheral, cardiovascular, and renal tissues (65–67). However, the present results do not indicate any significant interaction of BMAL1 with the E-box of the mouse *Agtrap* promoter (Fig. 4). This may be because the BMAL1-CLOCK heterodimer binds to multiple E-boxes of target genes despite there being a single E-box in the mouse *Agtrap* proximal promoter (66). The human *AGTRAP* promoter contains two adjacently located E-box motifs (Fig. 2). However, we did not obtain any evidence to indicate the interaction of BMAL1 with these two adjacently located E-box motifs in the *AGTRAP* promoter, at least in human kidney-derived cells (Fig. 7). Further studies are needed to examine the potential interaction of the BMAL1-CLOCK heterodimer with the adjacently located two E-box motifs in the *AGTRAP* promoter in other cells or tissues such as fat or liver, so as to exert cell type- or tissue-specific function. However, the results of the promoter assay and ChIP analysis clearly indicate the functional interactions of USF1/USF2 and the adjacently located two E-box motifs are involved in the regulation of the human *AGTRAP* promoter.

In summary, the results of this study show that Usf1 and Usf2 regulate *Agtrap* gene transcription through their interaction with the E-box in the mouse *Agtrap* promoter. Furthermore, the *in vitro* and *in vivo* results of siRNA transfection in mDCT cells and UUO in mice, respectively, suggest that Usf1 decreases and Usf2 increases *Agtrap* gene expression through the binding of Usf1/Usf2 to the E-box. We also demonstrated functional E-box-USF1/USF2 binding in the human *AGTRAP* promoter, thereby suggesting that a strategy of modulating the E-box-USF1/USF2 binding may have novel therapeutic potential.

REFERENCES

1. Mehta, P. K., and Griendling, K. K. (2007) Angiotensin II cell signaling: physiological and pathological effects in the cardiovascular system. *Am. J. Physiol. Cell Physiol.* **292,** C82–C97
2. Horiuchi, M., Iwanami, J., and Mogi, M. (2012) Regulation of angiotensin II receptors beyond the classical pathway. *Clin. Sci.* **123,** 193–203
3. Kobori, H., Nangaku, M., Navar, L. G., and Nishiyama, A. (2007) The intrarenal renin-angiotensin system: from physiology to the pathobiology of hypertension and kidney disease. *Pharmacol. Rev.* **59,** 251–287
4. Navar, L. G., Kobori, H., Prieto, M. C., and Gonzalez-Villalobos, R. A. (2011) Intratubular renin-angiotensin system in hypertension. *Hypertension* **57,** 355–362
5. Hein, L., Meinel, L., Pratt, R. E., Dzau, V. J., and Kobilka, B. K. (1997) Intracellular trafficking of angiotensin II and its AT1 and AT2 receptors: evidence for selective sorting of receptor and ligand. *Mol. Endocrinol.* **11,** 1266–1277
6. Miura, S., Saku, K., and Karnik, S. S. (2003) Molecular analysis of the structure and function of the angiotensin II type 1 receptor. *Hypertens. Res.* **26,** 937–943
7. Daviet, L., Lehtonen, J. Y., Tamura, K., Griese, D. P., Horiuchi, M., and Dzau, V. J. (1999) Cloning and characterization of ATRAP, a novel protein that interacts with the angiotensin II type 1 receptor. *J. Biol. Chem.* **274,** 17058–17062
8. Lopez-Ilasaca, M., Liu, X., Tamura, K., and Dzau, V. J. (2003) The angiotensin II type I receptor-associated protein, ATRAP, is a transmembrane protein and a modulator of angiotensin II signaling. *Mol. Biol. Cell* **14,** 5038–5050
9. Tanaka, Y., Tamura, K., Koide, Y., Sakai, M., Tsurumi, Y., Noda, Y., Umemura, M., Ishigami, T., Uchino, K., Kimura, K., Horiuchi, M., and Umemura, S. (2005) The novel angiotensin II type 1 receptor (AT1R)-associated protein ATRAP down-regulates AT1R and ameliorates cardiomyocyte hypertrophy. *FEBS Lett.* **579,** 1579–1586
10. Oshita, A., Iwai, M., Chen, R., Ide, A., Okumura, M., Fukunaga, S., Yoshii, T., Mogi, M., Higaki, J., and Horiuchi, M. (2006) Attenuation of inflammatory vascular remodeling by angiotensin II type 1 receptor-associated protein. *Hypertension* **48,** 671–676
11. Azuma, K., Tamura, K., Shigenaga, A., Wakui, H., Masuda, S., Tsurumi-Ikeya, Y., Tanaka, Y., Sakai, M., Matsuda, M., Hashimoto, T., Ishigami, T., Lopez-Ilasaca, M., and Umemura, S. (2007) Novel regulatory effect of angiotensin II type 1 receptor-interacting molecule on vascular smooth muscle cells. *Hypertension* **50,** 926–932
12. Mogi, M., Iwai, M., and Horiuchi, M. (2007) Emerging concepts of regulation of angiotensin II receptors: new players and targets for traditional receptors. *Arterioscler. Thromb. Vasc. Biol.* **27,** 2532–2539
13. Tamura, K., Tanaka, Y., Tsurumi, Y., Azuma, K., Shigenaga, A., Wakui, H., Masuda, S., and Matsuda, M. (2007) The role of angiotensin AT1 receptor-associated protein in renin-angiotensin system regulation and function. *Curr. Hypertens. Rep.* **9,** 121–127
14. Masuda, S., Tamura, K., Wakui, H., Maeda, A., Dejima, T., Hirose, T., Toyoda, M., Azuma, K., Ohsawa, M., Kanaoka, T., Yanagi, M., Yoshida, S., Mitsuhashi, H., Matsuda, M., Ishigami, T., Toya, Y., Suzuki, D., Nagashima, Y., and Umemura, S. (2010) Expression of angiotensin II type 1 receptor-interacting molecule in normal human kidney and IgA nephropathy. *Am. J. Physiol. Renal Physiol.* **299,** F720–F731
15. Wakui, H., Tamura, K., Matsuda, M., Bai, Y., Dejima, T., Shigenaga, A., Masuda, S., Azuma, K., Maeda, A., Hirose, T., Ishigami, T., Toya, Y., Yabana, M., Minamisawa, S., and Umemura, S. (2010) Intrarenal suppression of angiotensin II type 1 receptor binding molecule in angiotensin II-infused mice. *Am. J. Physiol. Renal Physiol.* **299,** F991–F1003
16. Wakui, H., Tamura, K., Tanaka, Y., Matsuda, M., Bai, Y., Dejima, T., Masuda, S., Shigenaga, A., Maeda, A., Mogi, M., Ichihara, N., Kobayashi, Y., Hirawa, N., Ishigami, T., Toya, Y., Yabana, M., Horiuchi, M., Minamisawa, S., and Umemura, S. (2010) Cardiac-specific activation of angiotensin II type 1 receptor-associated protein completely suppresses cardiac hypertrophy in chronic angiotensin II-infused mice. *Hypertension* **55,** 1157–1164
17. Tamura, K., Wakui, H., Maeda, A., Dejima, T., Ohsawa, M., Azushima, K., Kanaoka, T., Haku, S., Uneda, K., Masuda, S., Azuma, K., Shigenaga, A., Koide, Y., Tsurumi-Ikeya, Y., Matsuda, M., Toya, Y., Tokita, Y., Yamashita, A., and Umemura, S. (2013) The physiology and pathophysiology of a novel angiotensin receptor-binding protein ATRAP/Agtrap. *Curr. Pharm. Des.* **19,** 3043–3048
18. Shigenaga, A., Tamura, K., Wakui, H., Masuda, S., Azuma, K., Tsurumi-Ikeya, Y., Ozawa, M., Mogi, M., Matsuda, M., Uchino, K., Kimura, K., Horiuchi, M., and Umemura, S. (2008) Effect of olmesartan on tissue expression balance between angiotensin II receptor and its inhibitory binding molecule. *Hypertension* **52,** 672–678
19. Dejima, T., Tamura, K., Wakui, H., Maeda, A., Ohsawa, M., Kanaoka, T., Haku, S., Kengo, A., Masuda, S., Shigenaga, A., Azuma, K., Matsuda, M., Yabana, M., Hirose, T., Uchino, K., Kimura, K., Nagashima, Y., and Umemura, S. (2011) Prepubertal angiotensin blockade exerts long-term therapeutic effect through sustained ATRAP activation in salt-sensitive hypertensive rats. *J. Hypertens.* **29,** 1919–1929
20. Matsuda, M., Tamura, K., Wakui, H., Dejima, T., Maeda, A., Ohsawa, M., Kanaoka, T., Haku, S., Azushima, K., Yamasaki, H., Saito, D., Hirose, T., Maeshima, Y., Nagashima, Y., and Umemura, S. (2011) Involvement of Runx3 in the basal transcriptional activation of the mouse angiotensin II type 1 receptor-associated protein gene. *Physiol. Genomics* **43,** 884–894
21. Sawadogo, M., Van Dyke, M. W., Gregor, P. D., and Roeder, R. G. (1988) Multiple forms of the human gene-specific transcription factor USF. I. Complete purification and identification of USF from HeLa cell nuclei. *J. Biol. Chem.* **263,** 11985–11993
22. Sawadogo, M. (1988) Multiple forms of the human gene-specific transcription factor USF. II. DNA binding properties and transcriptional activity of the purified HeLa USF. *J. Biol. Chem.* **263,** 11994–12001
23. Gregor, P. D., Sawadogo, M., and Roeder, R. G. (1990) The adenovirus major late transcription factor USF is a member of the helix-loop-helix group of regulatory proteins and binds to DNA as a dimer. *Genes Dev.* **4,** 1730–1740
24. Sirito, M., Lin, Q., Maity, T., and Sawadogo, M. (1994) Ubiquitous expres-

sion of the 43- and 44-kDa forms of transcription factor USF in mammalian cells. *Nucleic Acids Res.* **22,** 427–433

25. Henrion, A. A., Vaulont, S., Raymondjean, M., and Kahn, A. (1996) Mouse USF1 gene cloning: comparative organization within the *c-myc* gene family. *Mamm. Genome* **7,** 803–809
26. Vallet, V. S., Henrion, A. A., Bucchini, D., Casado, M., Raymondjean, M., Kahn, A., and Vaulont, S. (1997) Glucose-dependent liver gene expression in upstream stimulatory factor 2−/− mice. *J. Biol. Chem.* **272,** 21944–21949
27. Vallet, V. S., Casado, M., Henrion, A. A., Bucchini, D., Raymondjean, M., Kahn, A., and Vaulont, S. (1998) Differential roles of upstream stimulatory factors 1 and 2 in the transcriptional response of liver genes to glucose. *J. Biol. Chem.* **273,** 20175–20179
28. Nowak, M., Helleboid-Chapman, A., Jakel, H., Martin, G., Duran-Sandoval, D., Staels, B., Rubin, E. M., Pennacchio, L. A., Taskinen, M. R., Fruchart-Najib, J., and Fruchart, J. C. (2005) Insulin-mediated down-regulation of apolipoprotein A5 gene expression through the phosphatidylinositol 3-kinase pathway: role of upstream stimulatory factor. *Mol. Cell. Biol.* **25,** 1537–1548
29. van Deursen, D., Jansen, H., and Verhoeven, A. J. (2008) Glucose increases hepatic lipase expression in HepG2 liver cells through up-regulation of upstream stimulatory factors 1 and 2. *Diabetologia* **51,** 2078–2087
30. Pajukanta, P., Lilja, H. E., Sinsheimer, J. S., Cantor, R. M., Lusis, A. J., Gentile, M., Duan, X. J., Soro-Paavonen, A., Naukkarinen, J., Saarela, J., Laakso, M., Ehnholm, C., Taskinen, M. R., and Peltonen, L. (2004) Familial combined hyperlipidemia is associated with upstream transcription factor 1 (USF1). *Nat. Genet.* **36,** 371–376
31. Ng, M. C., Miyake, K., So, W. Y., Poon, E. W., Lam, V. K., Li, J. K., Cox, N. J., Bell, G. I., and Chan, J. C. (2005) The linkage and association of the gene encoding upstream stimulatory factor 1 with type 2 diabetes and metabolic syndrome in the Chinese population. *Diabetologia* **48,** 2018–2024
32. Coon, H., Xin, Y., Hopkins, P. N., Cawthon, R. M., Hasstedt, S. J., and Hunt, S. C. (2005) Upstream stimulatory factor 1 associated with familial combined hyperlipidemia, LDL cholesterol, and triglycerides. *Hum. Genet.* **117,** 444–451
33. Sanchez, A. P., Zhao, J., You, Y., Declèves, A. E., Diamond-Stanic, M., and Sharma, K. (2011) Role of the USF1 transcription factor in diabetic kidney disease. *Am. J. Physiol. Renal Physiol.* **301,** F271–F279
34. Friedman, P. A., and Gesek, F. A. (1995) Stimulation of calcium transport by amiloride in mouse distal convoluted tubule cells. *Kidney Int.* **48,** 1427–1434
35. Gesek, F. A., and Friedman, P. A. (1995) Sodium entry mechanisms in distal convoluted tubule cells. *Am. J. Physiol.* **268,** F89–F98
36. Sakai, M., Tamura, K., Tsurumi, Y., Tanaka, Y., Koide, Y., Matsuda, M., Ishigami, T., Yabana, M., Tokita, Y., Hiroi, Y., Komuro, I., and Umemura, S. (2007) Expression of MAK-V/Hunk in renal distal tubules and its possible involvement in proliferative suppression. *Am. J. Physiol. Renal Physiol.* **292,** F1526–F1536
37. Tamura, K., Tanimoto, K., Murakami, K., and Fukamizu, A. (1992) A combination of upstream and proximal elements is required for efficient expression of the mouse renin promoter in cultured cells. *Nucleic Acids Res.* **20,** 3617–3623
38. Tamura, K., Umemura, S., Yamaguchi, S., Iwamoto, T., Kobayashi, S., Fukamizu, A., Murakami, K., and Ishii, M. (1994) Mechanism of cAMP regulation of renin gene transcription by proximal promoter. *J. Clin. Invest.* **94,** 1959–1967
39. Satoh, M., Kashihara, N., Yamasaki, Y., Maruyama, K., Okamoto, K., Maeshima, Y., Sugiyama, H., Sugaya, T., Murakami, K., and Makino, H. (2001) Renal interstitial fibrosis is reduced in angiotensin II type 1a receptor-deficient mice. *J. Am. Soc. Nephrol.* **12,** 317–325
40. Higuchi, R., Krummel, B., and Saiki, R. K. (1988) A general method of *in vitro* preparation and specific mutagenesis of DNA fragments: study of protein and DNA interactions. *Nucleic Acids Res.* **16,** 7351–7367
41. Kuipers, O. P., Boot, H. J., and de Vos, W. M. (1991) Improved site-directed mutagenesis method using PCR. *Nucleic Acids Res.* **19,** 4558
42. Tamura, K., Tanimoto, K., Ishii, M., Murakami, K., and Fukamizu, A. (1993) Proximal and core DNA elements are required for efficient angiotensinogen promoter activation during adipogenic differentiation. *J. Biol. Chem.* **268,** 15024–15032
43. Tsurumi, Y., Tamura, K., Tanaka, Y., Koide, Y., Sakai, M., Yabana, M., Noda, Y., Hashimoto, T., Kihara, M., Hirawa, N., Toya, Y., Kiuchi, Y., Iwai, M., Horiuchi, M., and Umemura, S. (2006) Interacting molecule of AT1 receptor, ATRAP, is colocalized with AT1 receptor in the mouse renal tubules. *Kidney Int.* **69,** 488–494
44. Dignam, J. D., Lebovitz, R. M., and Roeder, R. G. (1983) Accurate transcription initiation by RNA polymerase II in a soluble extract from isolated mammalian nuclei. *Nucleic Acids Res.* **11,** 1475–1489
45. Swick, A. G., Blake, M. C., Kahn, J. W., and Azizkhan, J. C. (1989) Functional analysis of GC element binding and transcription in the hamster dihydrofolate reductase gene promoter. *Nucleic Acids Res.* **17,** 9291–9304
46. Tamura, K., Chen, Y. E., Lopez-Ilasaca, M., Daviet, L., Tamura, N., Ishigami, T., Akishita, M., Takasaki, I., Tokita, Y., Pratt, R. E., Horiuchi, M., Dzau, V. J., and Umemura, S. (2000) Molecular mechanism of fibronectin gene activation by cyclic stretch in vascular smooth muscle cells. *J. Biol. Chem.* **275,** 34619–34627
47. Tamura, K., Chen, Y. E., Horiuchi, M., Chen, Q., Daviet, L., Yang, Z., Lopez-Ilasaca, M., Mu, H., Pratt, R. E., and Dzau, V. J. (2000) LXRα functions as a cAMP-responsive transcriptional regulator of gene expression. *Proc. Natl. Acad. Sci. U.S.A.* **97,** 8513–8518
48. Fukui, T., Rahman, M., Hayashi, K., Takeda, K., Higaki, J., Sato, T., Fukushima, M., Sakamoto, J., Morita, S., Ogihara, T., Fukiyama, K., Fujishima, M., and Saruta, T. (2003) Candesartan antihypertensive survival evaluation in Japan (CASE-J) trial of cardiovascular events in high-risk hypertensive patients: rationale, design, and methods. *Hypertens Res.* **26,** 979–990
49. Basbous, J., Arpin, C., Gaudray, G., Piechaczyk, M., Devaux, C., and Mesnard, J. M. (2003) The HBZ factor of human T-cell leukemia virus type I dimerizes with transcription factors JunB and c-Jun and modulates their transcriptional activity. *J. Biol. Chem.* **278,** 43620–43627
50. Carabana, J., Ortigoza, E., and Krangel, M. S. (2005) Regulation of the murine Dδ2 promoter by upstream stimulatory factor 1, Runx1, and c-Myb. *J. Immunol.* **174,** 4144–4152
51. Lim, M., Zhong, C., Yang, S., Bell, A. M., Cohen, M. B., and Roy-Burman, P. (2010) Runx2 regulates survivin expression in prostate cancer cells. *Lab. Invest.* **90,** 222–233
52. Purvis, T. L., Hearn, T., Spalluto, C., Knorz, V. J., Hanley, K. P., Sanchez-Elsner, T., Hanley, N. A., and Wilson, D. I. (2010) Transcriptional regulation of the Alström syndrome gene ALMS1 by members of the RFX family and Sp1. *Gene* **460,** 20–29
53. Bu, Y., and Gelman, I. H. (2007) v-Src-mediated down-regulation of SSeCKS metastasis suppressor gene promoter by the recruitment of HDAC1 into a USF1-Sp1-Sp3 complex. *J. Biol. Chem.* **282,** 26725–26739
54. Zhu, Y., Casado, M., Vaulont, S., and Sharma, K. (2005) Role of upstream stimulatory factors in regulation of renal transforming growth factor-β1. *Diabetes* **54,** 1976–1984
55. Liu, S., Shi, L., and Wang, S. (2007) Overexpression of upstream stimulatory factor 2 accelerates diabetic kidney injury. *Am. J. Physiol. Renal Physiol.* **293,** F1727–F1735
56. Shi, L., Nikolic, D., Liu, S., Lu, H., and Wang, S. (2009) Activation of renal renin-angiotensin system in upstream stimulatory factor 2 transgenic mice. *Am. J. Physiol. Renal Physiol.* **296,** F257–F265
57. Dickson, M. E., Tian, X., Liu, X., Davis, D. R., and Sigmund, C. D. (2008) Upstream stimulatory factor is required for human angiotensinogen expression and differential regulation by the A-20C polymorphism. *Circ. Res.* **103,** 940–947
58. Park, S., Liu, X., Davis, D. R., and Sigmund, C. D. (2012) Gene trapping uncovers sex-specific mechanisms for upstream stimulatory factors 1 and 2 in angiotensinogen expression. *Hypertension* **59,** 1212–1219
59. Viollet, B., Lefrançois-Martinez, A. M., Henrion, A., Kahn, A., Raymondjean, M., and Martinez, A. (1996) Immunochemical characterization and transacting properties of upstream stimulatory factor isoforms. *J. Biol. Chem.* **271,** 1405–1415
60. Sirito, M., Lin, Q., Deng, J. M., Behringer, R. R., and Sawadogo, M. (1998) Overlapping roles and asymmetrical cross-regulation of the USF proteins in mice. *Proc. Natl. Acad. Sci. U.S.A.* **95,** 3758–3763
61. Jiang, B., and Mendelson, C. R. (2003) USF1 and USF2 mediate inhibition

of human trophoblast differentiation and CYP19 gene expression by Mash-2 and hypoxia. *Mol. Cell. Biol.* **23,** 6117–6128

62. Ma, Z., Jhun, B., Jung, S. Y., and Oh, C. K. (2008) Binding of upstream stimulatory factor 1 to the E-box regulates the 4G/5G polymorphism-dependent plasminogen activator inhibitor 1 expression in mast cells. *J. Allergy Clin. Immunol.* **121,** 1006–1012
63. Olave, N. C., Grenett, M. H., Cadeiras, M., Grenett, H. E., and Higgins, P. J. (2010) Upstream stimulatory factor-2 mediates quercetin-induced suppression of PAI-1 gene expression in human endothelial cells. *J. Cell Biochem.* **111,** 720–726
64. Chen, B., Hsu, R., Li, Z., Kogut, P. C., Du, Q., Rouser, K., Camoretti-Mercado, B., and Solway, J. (2012) Upstream stimulatory factor 1 activates GATA5 expression through an E-box motif. *Biochem. J.* **446,** 89–98
65. Schoenhard, J. A., Smith, L. H., Painter, C. A., Eren, M., Johnson, C. H., and Vaughan, D. E. (2003) Regulation of the PAI-1 promoter by circadian clock components: differential activation by BMAL1 and BMAL2. *J. Mol. Cell. Cardiol.* **35,** 473–481
66. Ripperger, J. A., and Schibler, U. (2006) Rhythmic CLOCK-BMAL1 binding to multiple E-box motifs drives circadian Dbp transcription and chromatin transitions. *Nat. Genet.* **38,** 369–374
67. Saifur Rohman, M., Emoto, N., Nonaka, H., Okura, R., Nishimura, M., Yagita, K., van der Horst, G. T., Matsuo, M., Okamura, H., and Yokoyama, M. (2005) Circadian clock genes directly regulate expression of the Na^+/H^+ exchanger NHE3 in the kidney. *Kidney Int.* **67,** 1410–1419

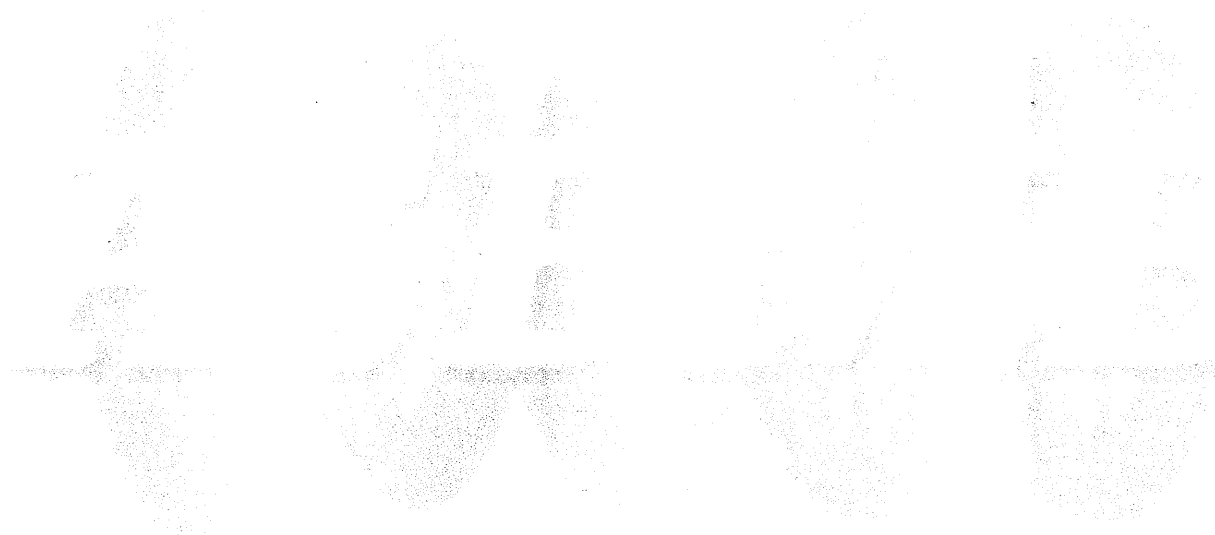

Therapeutic Apheresis and Dialysis

Therapeutic Apheresis and Dialysis 2013; 17(2):185–192
doi: 10.1111/j.1744-9987.2012.01149.x

Therapeutic Potential of Low-Density Lipoprotein Apheresis in the Management of Peripheral Artery Disease in Patients With Chronic Kidney Disease

Kouichi Tamura,[1] Yuko Tsurumi-Ikeya,[1] Hiromichi Wakui,[1] Akinobu Maeda,[1] Masato Ohsawa,[1] Kengo Azushima,[1] Tomohiko Kanaoka,[1] Kazushi Uneda,[1] Sona Haku,[1] Koichi Azuma,[2] Hiroshi Mitsuhashi,[3] Nobuko Tamura,[4] Yoshiyuki Toya,[1] Yasuo Tokita,[5] Toshiharu Kokuho,[6] and Satoshi Umemura[1]

[1]Department of Medical Science and Cardiorenal Medicine, Yokohama City University Graduate School of Medicine, [2]Department of Medicine, Yokohama Dai-ichi Hospital of Zenjin Foundation, [3]Department of Nephrology and Hypertension, Yokohama Minami-Kyosai Hospital, [4]Department of Dermatology, Kanagawa Prefecture Shiomidai Hospital, Yokohama, [5]Renal Division, Department of Medicine, Fujisawa Municipal Hospital, Fujisawa, and [6]Department of Nephrology and Hypertension, Yokosuka City Hospital, Yokosuka, Japan

Abstract: Cardiovascular disease (CVD) is a major cause of death in patients with chronic kidney disease (CKD). Patients with CKD are reported to have a significant greater risk of CVD-associated mortality than that of the general population after stratification for age, gender, race, and the presence or absence of diabetes. CKD itself is also an independent risk factor for the development of atherosclerosis, and in particular, patients undergoing dialysis typically bear many of the risk factors for atherosclerosis, such as hypertension, dyslipidemia and disturbed calcium-phosphate metabolism, and commonly suffer from severe atherosclerosis, including peripheral arterial disease (PAD). Low-density lipoprotein (LDL) apheresis is a potentially valuable treatment applied to conventional therapy-resistant hypercholesterolemic patients with coronary artery disease and PAD. Although previous and recent studies have suggested that LDL apheresis exerts beneficial effects on the peripheral circulation in dialysis patients suffering from PAD, probably through a reduction of not only serum lipids but also of inflammatory or coagulatory factors and oxidative stress, the precise molecular mechanisms underlying the long-term effects of LDL apheresis on the improvement of the peripheral circulation remains unclear and warrants further investigation. **Key Words:** Chronic kidney disease, Hemodialysis patients, Low-density lipoprotein apheresis, Oxidative stress, Peripheral artery disease.

Cardiovascular disease (CVD) has a major effect on the prognosis of patients with chronic kidney disease (CKD), particularly for those patients on dialysis, and atherosclerotic vascular changes play a critical role. Renal deterioration in CKD promotes hypertension, dyslipidemia, insulin resistance, disturbed calcium-phosphate metabolism and renal anemia, and these are all risk factors for atherosclerosis. In addition, chronic inflammation, oxidative stress and variability in blood pressure and circulating blood volume also promote atherosclerotic vascular changes in dialysis CKD patients. Among the systemic atherosclerotic vascular diseases, peripheral arterial disease (PAD) is prevalent in dialysis CKD patients. In dialysis CKD patients, the PAD lesions are prone to being distributed in the arteries of the lower limbs and exhibit a severely stenotic lumen

Received June 2012; revised September 2012.
Address correspondence and reprint requests to Dr Kouichi Tamura, Department of Medical Science and Cardiorenal Medicine, Yokohama City University Graduate School of Medicine, 3-9 Fukuura, Kanazawa-ku, Yokohama 236-0004, Japan. Email: tamukou@med.yokohama-cu.ac.jp
Presented in part at the 7th Lipidclub & Therapeutic Apheresis Satellite Symposium of the 80th European Atherosclerosis Society Congress held May 23–24, 2012 in San Gemini, Italy.

with vascular calcification without the development of any collateral circulation, and patients with CKD and PAD have higher mortality rates than those with either of these conditions alone (1).

Percutaneous transluminal angioplasty (PTA) for the treatment of PAD is reported to suffer from the problem of an increased rate of restenosis in dialysis CKD patients (2). PAD in HD patients is often therapy resistant and closely associated with an increased risk of cardiovascular mortality, morbidity, and hospitalization as well as a reduced Health-Related Quality of Life (HRQOL), even after bypass surgery and leg amputation (3,4). In certain countries, including most of the countries in Europe, LDL apheresis is the treatment of choice in patients with homozygous familial hypercholesterolemia (FH), particularly those refractory to statins, as described in a recent review (5). LDL apheresis has been shown to exert beneficial effects on aortic and coronary atherosclerosis and to reduce the risk of coronary artery disease in patients with homozygous FH (6,7). Recently LDL apheresis has become the adjuvant treatment of choice for dialysis CKD patients with PAD, particularly those refractory to statins and on whom it is difficult to perform PTA or bypass surgery (8,9). In this review we briefly summarize the clinical applications of LDL apheresis in Japan and mechanistic basis for its benefit in PAD in dialysis patients.

PRESENT INDICATION OF LDL APHERESIS FOR THERAPY OF PAD IN JAPAN

In Japan, indicated usage of LDL apheresis for the treatment of PAD under the government system of insurance coverage, includes the following. (i) clinical signs of poor peripheral circulation, such as cold, decolored or ulcerated extremities, or intermittent claudication consistent with a Fontaine classification of Grade II or more; (ii) refractoriness to conventional medical or surgical treatment; (iii) an excessively high LDL cholesterol (LDL-C) or total cholesterol (TC) levels (LDL-C >140 mg/dL or TC >220 mg/dL) in spite of drug treatment (10). Japanese government insurance coverage permits 10 sessions of LDL apheresis for each patient to be carried out during a 3-month period.

THE PATHOGENESIS OF LIPOPROTEIN ABNORMALITIES IN CKD

Although hypercholesterolemia is a major requisite for the governmental insurance-covered application of LDL apheresis for the treatment of PAD in Japan, the regulatory system of lipid metabolism is reported to be highly disturbed in CKD patients, owing to alterations in apolipoproteins, lipid transfer proteins, lipolytic enzymes and lipoprotein receptors (11,12). Previous studies demonstrated that LDL particles are heterogeneous with respect to their size, density and lipid composition (13,14). Among the LDL particles, the smaller and denser LDL particles (small dense low-density LDL particles) are more atherogenic (13), and the small dense low-density LDL phenotype is strongly associated with the development of coronary heart disease (15).

In CKD patients, triglyceride concentrations increase while HDL cholesterol (HDL-C) concentrations decline, and there is a progressive accumulation of the more atherogenic, small dense low-density LDL particles, in spite of low-to-normal TC and LDL-C levels (11). In addition, in dialysis CKD patients, dyslipidemia is typified by a marked increase in triglyceride-rich apo B-containing particles, a decreased HDL concentration and a predominance of small dense LDL particles, with a normal LDL-C level but an increased lipoprotein(a) (Lp[a]) concentration. Also, there is reportedly a persistent disturbance in the apolipoprotein profile, with reduced apo AI and apo AII concentrations and significant increases in the apoB, apoCIII and apoE concentrations (11,16).

LDL APHERESIS FOR THE TREATMENT OF PAD

There are presently several systems of LDL apheresis in use, including cascade and lipid filtration, immunoadsorption, heparin-induced LDL precipitation, dextran sulfate LDL adsorption, and the LDL hemoperfusion (17,18). In Japan, LDL apheresis therapy using the strategy of LDL absorption with dextran sulfate (Liposorber LA-15, Kaneka, Japan) is most commonly performed (19,20). Low-molecular dextran sulfate (MW 4500) selectively absorbs all substances containing apoB. The binding mechanism is the direct interaction between the dextran sulfate and the positively charged surface of apoB-containing lipoproteins (LDL-C, very low density lipoprotein-cholesterol [VLDL-C], and Lp[a]). Dextran sulfate has a structure similar to that of the LDL receptor and seems to act as a type of pseudoreceptor. Approximately 2.5 g LDL-C can be bound per column. After primary separation, the plasma is perfundated through the columns, where all material containing apoB such as cholesterol, LDL-C, VLDL-C, and triglycerides is absorbed, but without any absorption of HDL-C, which does not contain apoB (18).

In our hospital, LDL apheresis is performed using hollow polysulfone fibers (Sulflux, Kaneka, Osaka, Japan) as the plasma separator and a dextran sulfate cellulose column (Liposorber LA-15, Kaneka) as the LDL absorber. Blood flow from the A-V fistula access in the case of dialysis CKD patients is typically in the range of 80–100 mL/min, the plasma flow is 25–30 mL/min, and 3000–4000 mL of the plasma volume is treated per session. Heparin or nafamostat mesilate is given as an anticoagulant for extracorporeal circulation. To maintain good adsorption efficiency with an increasing quantity of plasma treated, two columns arranged in a row are used in turn automatically, so that one column can be washed with the specific liquid and regenerated after the treatment of the plasma while the other is in operation (MA-03 system, Kaneka) (21,22). LDL apheresis is carried out once or twice a week on non-HD days in the case of dialysis CKD patients, and 10 sessions of apheresis are performed in each patient.

THERAPEUTIC EFFECTS OF LDL APHERESIS IN DIALYSIS CKD PATIENTS WITH PAD

Although dialysis CKD patients with PAD often exhibit low-to-normal TC and LDL-C levels along with increased triglycerides and reduced HDL-C levels, previous studies showed that LDL apheresis by the dextran sulfate cellulose column (Liposorber LA-15, Kaneka) is clinically effective even in PAD patients undergoing HD (23–28). Since PAD patients undergoing HD tend to be resistant to any treatment and are at high risk for lower-extremity amputation, LDL apheresis is suggested to be a useful strategy in the multidisciplinary approach for therapy of PAD (Fig. 1).

In a recent clinical study we conducted, 25 dialysis CKD patients with PAD were enrolled, and the therapeutic effects of LDL apheresis in 19 patients were ultimately analyzed (22). Blood samples were collected before and after the first session, at the start of the 10th session, and at 3 months after the end of treatment (before regular HD). The absolute walking distance and ankle-brachial pressure index (ABI) were principally estimated on non-HD days prior to the 1st and 10th sessions and at 3 months after the end of treatment, and the long-term periods in this study were defined as the time from the 1st session to the 10th session and the time from the 1st session up to the third month after the end of the 10th sessions.

Because most of these patients were unable to perform treadmill exercise because of conditions such as a previous heart attack or paralysis, the absolute walking distance was evaluated by medical staff on a flat floor in the hospital. Of the 25 patients enrolled, five patients could not complete the study because of death ($N = 3$), amputation ($N = 1$) or PTA ($N = 1$) during the study period, and they were excluded from the analysis. On the whole, the absolute walking distance improved significantly by the 10th session of LDL apheresis compared with baseline and was still improved even at 3 months after the end of the treatment (Table 1) (22). Similarly, the ABI was improved by the 10th session compared with baseline (Table 1). Subsequently, the patients were classified into two groups according to the changes in the ABI at 3 months after the end of

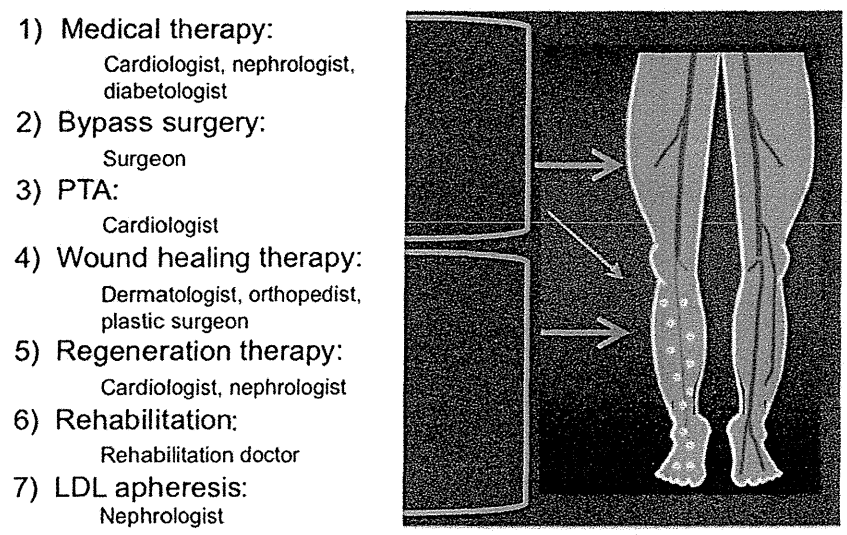

FIG. 1. Multidisciplinary therapeutic approach to peripheral arterial disease (PAD) in Japan.

TABLE 1. *Therapeutic effects of low density lipoprotein (LDL) apheresis in dialysis chronic kidney disease (CKD) patients with peripheral arterial disease (PAD)*

Clinical parameters	Baseline	After 1st apheresis	At 10th apheresis	3 months after 10th apheresis	*P1*	*P2*	*P3*
Total patients ($N = 19$):							
Walking distance (m)	171 ± 33	N/A	294 ± 34	270 ± 42	N/A	<0.05	<0.05
ABI	0.59 ± 0.04	N/A	0.67 ± 0.04	0.64 ± 0.04	N/A	<0.05	NS
ABI responders ($N = 10$):							
Walking distance (m)	118 ± 26	N/A	333 ± 45	297 ± 63	N/A	<0.05	<0.05
ABI	0.53 ± 0.06	N/A	0.69 ± 0.06	0.69 ± 0.05	N/A	<0.005	<0.005
LDL cholesterol (mg/dL)	88 ± 7	32 ± 3	78 ± 9	98 ± 11	<0.01	NS	NS
Oxidized LDL (U/L)	38 ± 3	20 ± 2	32 ± 3	38 ± 4	<0.01	<0.05	NS
Fibrinogen (mg/dL)	400 ± 14	308 ± 18	337 ± 32	394 ± 35	<0.01	0.07	NS
CRP (mg/dL)	0.87 ± 0.40	0.49 ± 0.20	0.39 ± 0.23	0.75 ± 0.47	<0.05	0.07	NS
ABI non-responders ($N = 9$):							
Walking distance (m)	232 ± 58	N/A	254 ± 49	238 ± 59	N/A	NS	NS
ABI	0.65 ± 0.05	N/A	0.63 ± 0.05	0.59 ± 0.06	N/A	NS	NS
LDL cholesterol (mg/dL)	83 ± 8	26 ± 2	75 ± 10	104 ± 16	<0.05	NS	NS
Oxidized LDL (U/L)	38 ± 5	18 ± 2	32 ± 4	46 ± 6	<0.05	NS	<0.05
Fibrinogen (mg/dL)	388 ± 38	264 ± 28	340 ± 45	427 ± 35	<0.05	NS	NS
CRP (mg/dL)	0.81 ± 0.47	0.34 ± 0.21	1.12 ± 1.02	0.61 ± 0.35	<0.05	NS	NS

Parameters are shown as the mean ± standard error. *P1* indicates the baseline vs. after the 1st apheresis; *P2*, the baseline vs. at the 10th apheresis; *P3*, the baseline vs. 3 months after the 10th apheresis (Modified from Tsurumi-Ikeya Y et al. *Arterioscler Thromb Vasc Biol* 2010;30:1058–1065). ABI, ankle-brachial pressure index; CRP, C-reactive protein; N/A, not applicable; NS, not significant.

treatment. The two groups were patients with an improved ABI (ABI responders, $N = 10$) and patients with a worsened ABI (ABI non-responders, $N = 9$). The serum levels of LDL-C and oxidized LDL, along with the C-reactive protein (CRP) and fibrinogen concentrations were significantly reduced after a single session in both groups. However, in the responders, LDL apheresis showed a trend toward a long-term reduction of the circulating levels of oxidized LDL, CRP, and fibrinogen (Table 1), in addition to a short-term dramatic decrease in the TC and LDL-C levels after each LDL apheresis session (Table 1).

When the baseline parameters of the ABI responders and non-responders were compared in order to analyze factors involved in the therapeutic effects of LDL apheresis, the walking distance as well as ABI tended to be lower in the ABI responders than in the ABI non-responders (walking distance, 118 ± 26 vs. 232 ± 58 m, $P = 0.08$; ABI, 0.53 ± 0.06 vs. 0.65 ± 0.05, $P = 0.12$), thereby suggesting that dialysis CKD patients with severe symptoms of PAD may be afforded a long-term therapeutic benefit by LDL apheresis. However, although the absolute walking distance and ABI still remained significantly improved in the responders 3 months after the tenth apheresis compared to these parameters at baseline, the LDL apheresis-mediated decrease in the oxidized LDL, CRP and fibrinogen concentrations lasted until just after the tenth apheresis, but not at 3 months after the tenth apheresis. Thus, there is a discrepancy between the long-term therapeutic effects of LDL apheresis on the clinical parameters of the walking distance and ABI, and the improvements in the laboratory parameters, including oxidized LDL, CRP and fibrinogen.

Thus, in order to examine the mechanism by which the absolute walking distance and ABI improved, even though the LDL apheresis did not result in a decrease in either oxidized LDL or inflammation at 3 months after the tenth apheresis, additional statistical correlation analyses were performed (Fig. 2) (22). As a result, there were statistically significant correlations between the walking distance and the plasma oxidized LDL ($R = -0.448$, $P < 0.05$, Fig. 2A) and fibrinogen ($R = -0.779$, $P < 0.05$, Fig. 2B) levels in the responders. In the non-responders, there was only a marginal correlation between the walking distance and the plasma oxidized LDL ($R = -0.329$, $P = 0.07$, Fig. 2C). Therefore, the therapeutic effects of LDL apheresis appear to be related to a chronic reduction of oxidized LDL and fibrinogen, as revealed by the significant negative relationships between the walking distance and the laboratory parameters.

Nevertheless, one of the obvious limitations of this study is the small number of enrolled patients. In addition, most of the patients were unable to perform treadmill exercise because of conditions such as previous heart attack or paralysis, but these are two distinctly different pathologies. Thus, although there should be at least four groups, that is, responders and non-responders in patients with heart attack and those with paralysis, respectively, to be strictly correct for the purposes of analysis, this was not possible due

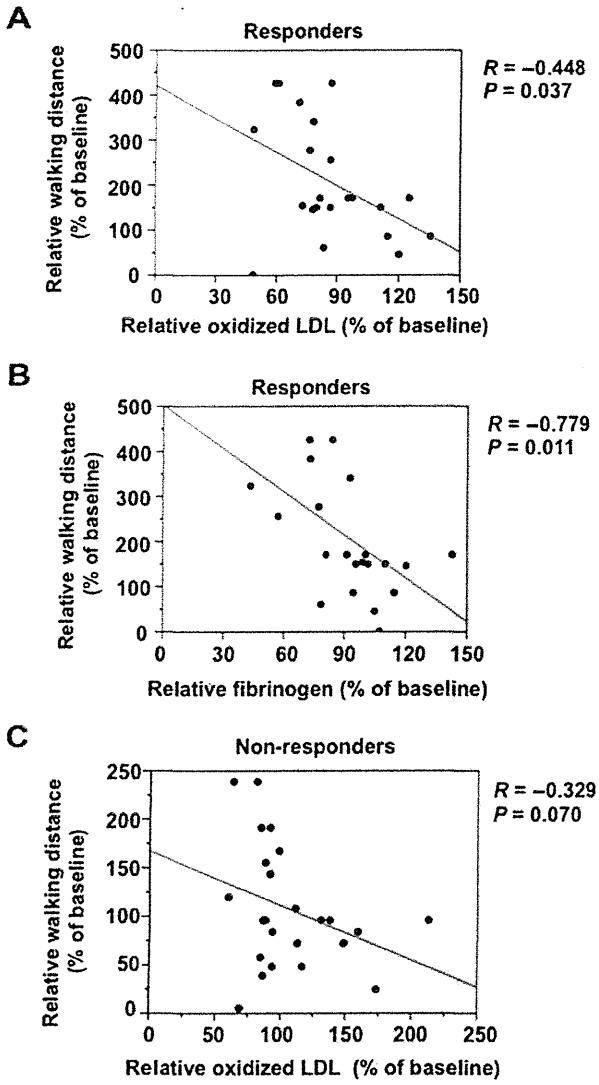

FIG. 2. Relationships between the walking distance (relative walking distance) and plasma oxidized low density lipoprotein (LDL) (relative oxidized LDL) (A), fibrinogen (relative fibrinogen) levels (B) in the responders, and between the walking distance (relative walking distance) and plasma oxidized LDL (relative oxidized LDL) (C) in the non-responders. The respective values were calculated relative to those achieved at baseline in either the responder group or the non-responder group (Modified from Tsurumi-Ikeya Y et al. *Arterioscler Thromb Vasc Biol* 2010; 30: 1058–65).

to the limited number and type of patients available. Furthermore, there is a possibility that other factor(s), which have not been identified in these studies, play a critical role in mediating the long-term therapeutic effects of LDL apheresis in CKD patients with PAD. Also, the components of the non-responders' serum responsible for the insufficient clinical improvement remain to be determined. Therefore, further studies, such as investigations using mass spectrometry, are needed (29).

MECHANISMS INVOLVED IN THE THERAPEUTIC EFFECTS OF LDL APHERESIS IN DIALYSIS CKD PATIENTS WITH PAD

Low density lipoprotein apheresis not only improves clinical symptoms rapidly, but also results in sustained improvement, although the mechanism has not been fully elucidated. Recently, LDL-C crystals in the phagosome of vascular macrophages were shown to directly activate Nod-like receptor family, pyrin domain–containing 3 (NLRP3) inflammasomes and thus to trigger atherogenesis in the early phase (30,31), and previous studies demonstrated that a single LDL apheresis decreased not only the TC and LDL-C concentrations, but also the oxidized LDL-C, CRP and fibrinogen concentrations in the short term (18). Dialysis CKD patients are reportedly characterized by higher levels of oxidative and inflammation than healthy subjects (11,32–34). Oxidative stress and inflammation are correlated strongly with tryglycerides, VLDL-C, apoC-III and apoC-III bound to apoB-containing lipoproteins, but not with either TC or LDL-C (35).

With respect to the long-term effects of LDL apheresis on lipid-related oxidative stress, a previous study has shown both acute and chronic effects of LDL apheresis in lowering the susceptibility of LDL to oxidation in non-CKD patients with severe, genetically determined hypercholesterolemia (36). In our previous study, the therapeutic effects of LDL apheresis were related to the relatively sustained decrease in oxidized LDL and fibrinogen, which are markers of lipid peroxidation and blood coagulation, respectively (Table 1, Fig. 2) (22). Other studies also showed LDL apheresis-mediated reduction of thiobarbituric acid-reactive substances, thiobarbituric acid being a marker of lipid peroxidation, and also a production of reactive oxygen species via the suppression of nicotinamide adenine dinucleotide phosphate (NADPH) oxidase expression in leukocytes in HD patients (28). Therefore, these results suggest that LDL apheresis-mediated suppression of lipid peroxidation is one of the contributing factors to its therapeutic effect on the peripheral circulation in end-stage renal disease patients with PAD. Other potential mechanisms have also been proposed to play a role in the therapeutic effects of LDL apheresis on atherosclerotic vascular lesions (Table 2).

The therapeutic effects of LDL apheresis on the inflammatory profile have also been reported. Stefanutti et al. showed that LDL apheresis resulted in an anti-inflammatory and anti-atherogenic cytokine profile in the plasma of non-CKD patients with

TABLE 2. *Proposed effects of low density lipoprotein (LDL) apheresis*

- Reduction of whole blood and plasma viscosity
- Improvement of red blood cells (deformability)
- Increase of vasodilation factors (bradykinin, NO, PGI_2)
- Reduction of coagulation factors (fibrinogen etc.)
- Reduction of cell adhesion factors (ICAM-1, ELAM-1etc.)
- Reduction of CRP and MMP-9
- Inhibition of platelet activation
- Increase of HGF and endothelial progenitor cells

CRP, C-reactive protein; ELAM-1, endothelial leukocyte adhesion molecule-1 (E-selectin); HGF, hepatocyte growth factor; ICAM-1, intercellular adhesion molecule-1; MMP-9, matrix metalloproteinase-9; NO, nitric oxide; PGI_2, prostacyclin.

severe dyslipidemia and pre-existing angiographically demonstrated atherosclerotic lesions, that is, those patients at the highest level of individual cardiovascular risk (37). In another previous study, several cytokines and complement activation products, which are important for the progression of vascular atherosclerosis as well as plaque instability, were differently affected by the three apheresis columns DL-75 (whole blood adsorption), LA-15 (plasma adsorption), and EC-50W (plasma filtration) (38). This was true even in cases in which the LDL-C was reduced equally by all of them, and the adsorption columns displayed an apparently more beneficial inflammatory profile than the filtration device (38).

Vascular endothelial cells play important preventive roles against the development of atherosclerotic vascular disease (39). Previous studies showed that a single LDL apheresis session enhanced the peripheral microcirculation, probably by increasing the production of nitric oxide (NO) and bradykinin (40), reducing blood viscosity and adhesion molecules (41), and inducing endothelium-dependent vasodilatation (42). Another study demonstrated that endothelium-dependent vasodilation was significantly increased even 4 weeks after the final LDL apheresis in dialysis CKD patients with PAD (26). Thus, to investigate the molecular mechanism involved in the long-term therapeutic effects of LDL apheresis on endothelial cells, we examined the effects of LDL apheresis on vascular endothelial cell functions in vitro by analyzing the expression of the activated form of endothelial nitric oxide synthase (eNOS), which is phosphorylated at Ser-1177 (43), and cellular proliferative activity (22). The expression of the activated eNOS protein in human umbilical vein endothelial cells (HUVECs) was significantly increased by incubation with the serum from the responders at the 10th session compared with the serum collected after the first apheresis (22). Furthermore, the proliferative activity of HUVECs was increased by the serum collected from the responders at 3 months after the end of treatment (22). Collectively, these results suggest that the therapeutic effects of LDL apheresis on CKD patients with PAD are at least partly dependent on the sustained reduction of oxidized LDL-C and fibrinogen, along with the activated eNOS-mediated improvement of endothelial cell function (Fig. 3). Because the

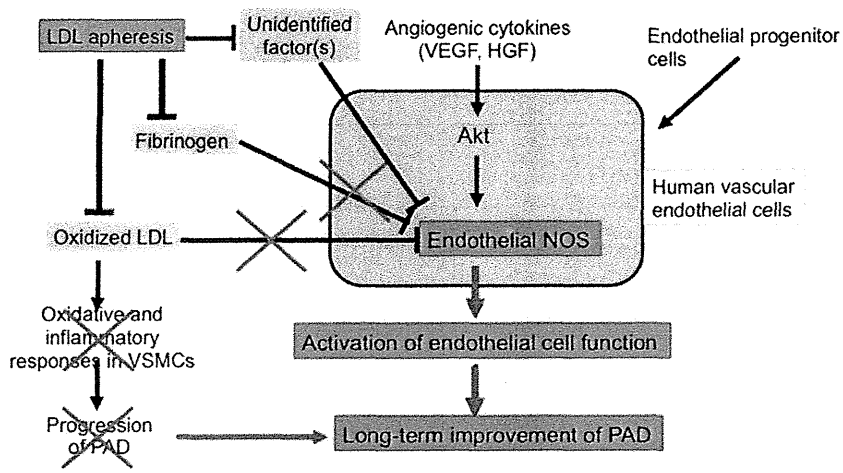

FIG. 3. Low density lipoprotein (LDL) apheresis exerts long-term therapeutic effects on peripheral arterial disease (PAD) in chronic kidney disease (CKD) patients, at least partly via a sustained reduction of oxidized LDL and fibrinogen, along with an activated endothelial nitric oxide synthase (eNOS)-mediated improvement of endothelial cell function. There is a possibility that other factor(s), which have not been identified yet, may play a critical role in mediating the therapeutic effects of LDL apheresis on endothelial cellular function. Further efforts, such as microarray analysis, are needed to identify the precise molecular mechanism of the LDL apheresis-mediated effects on endothelial cells and to improve the therapeutic efficacy of LDL apheresis. HGF, hepatocyte growth factor; PAD, peripheral arterial disease; VEGF, vascular endothelial growth factor; VSMCs, vascular smooth muscle cells.

activation of endothelial cells is an important strategy for the amelioration of the atherosclerotic vascular process (39) and there is a possibility that other factor(s), which have not been identified yet, play a critical role in mediating the therapeutic effects of LDL apheresis on endothelial cellular function, further investigative efforts, such as microarray analysis, should be used to identify the precise molecular mechanism of the LDL apheresis-mediated effects on endothelial cells and to improve the therapeutic efficacy of LDL apheresis (44).

Acknowledgments: This review was supported in part by grants from the Japanese Ministry of Education, Science, Sports and Culture, by Health and Labor Sciences Research grant; and by grants from Salt Science Research Foundation (No. 1134), the Kidney Foundation, Japan (JKFB11-25) and Novartis Foundation for Gerontological Research (2012). Pacific Edit reviewed the manuscript prior to submission.

REFERENCES

1. Garimella PS, Hart PD, O'Hare A, Deloach S, Herzog CA, Hirsch AT. Peripheral artery disease and CKD: a focus on peripheral artery disease as a critical component of CKD care. *Am J Kidney Dis* 2012;60:641–54.
2. Kumada Y, Aoyama T, Ishii H et al. Long-term outcome of percutaneous transluminal angioplasty in chronic haemodialysis patients with peripheral arterial disease. *Nephrol Dial Transplant* 2008;23:3996–4001.
3. Rajagopalan S, Dellegrottaglie S, Furniss AL et al. Peripheral arterial disease in patients with end-stage renal disease: observations from the Dialysis Outcomes and Practice Patterns Study (DOPPS). *Circulation* 2006;114:1914–22.
4. Weis-Muller BT, Rommler V, Lippelt I et al. Critical chronic peripheral arterial disease: does outcome justify crural or pedal bypass surgery in patients with advanced age or with comorbidities? *Ann Vasc Surg* 2011;25:783–95.
5. Raal FJ, Santos RD. Homozygous familial hypercholesterolemia: current perspectives on diagnosis and treatment. *Atherosclerosis* 2012;223:262–8.
6. Mabuchi H, Koizumi J, Shimizu M et al. Long-term efficacy of low-density lipoprotein apheresis on coronary heart disease in familial hypercholesterolemia. Hokuriku-FH-LDL-Apheresis Study Group. *Am J Cardiol* 1998;82:1489–95.
7. Thompson GR. Recommendations for the use of LDL apheresis. *Atherosclerosis* 2008;198:247–55.
8. Agishi T, Kitano Y, Suzuki T et al. Improvement of peripheral circulation by low density lipoprotein adsorption. *ASAIO Trans* 1989;35:349–51.
9. Inoue I, Takahashi K, Kikuchi C, Katayama S. LDL apheresis reduces the susceptibility of LDL to in vitro oxidation in a diabetic patient with hemodialysis treatment. *Diabetes Care* 1996;19:1103–7.
10. Naganuma S, Agishi T, Ota K. LDL apheresis in atherosclerotic disease with hyperlipidemia. *ASAIO J* 1992;38:M436–9.
11. Chan DT, Irish AB, Dogra GK, Watts GF. Dyslipidaemia and cardiorenal disease: mechanisms, therapeutic opportunities and clinical trials. *Atherosclerosis* 2008;196:823–34.
12. Nitta K. Clinical assessment and management of dyslipidemia in patients with chronic kidney disease. *Clin Exp Nephrol* 2012;16:522–9.
13. Bjornheden T, Babyi A, Bondjers G, Wiklund O. Accumulation of lipoprotein fractions and subfractions in the arterial wall, determined in an in vitro perfusion system. *Atherosclerosis* 1996;123:43–56.
14. Hirano T, Ito Y, Yoshino G. Measurement of small dense low-density lipoprotein particles. *J Atheroscler Thromb* 2005; 12:67–72.
15. Austin MA, Breslow JL, Hennekens CH, Buring JE, Willett WC, Krauss RM. Low-density lipoprotein subclass patterns and risk of myocardial infarction. *JAMA* 1988;260:1917–21.
16. Fytili CI, Progia EG, Panagoutsos SA et al. Lipoprotein abnormalities in hemodialysis and continuous ambulatory peritoneal dialysis patients. *Ren Fail* 2002;24:623–30.
17. Hequet O, Le QH, Rigal D et al. The first results demonstrating efficiency and safety of a double-column whole blood method of LDL-apheresis. *Transfus Apher Sci* 2010;42:3–10.
18. Bambauer R, Bambauer C, Lehmann B, Latza R, Schiel R. LDL-apheresis: technical and clinical aspects. *ScientificWorldJournal* 2012;2012:314283.
19. Mabuchi H, Michishita I, Takeda M et al. A new low density lipoprotein apheresis system using two dextran sulfate cellulose columns in an automated column regenerating unit (LDL continuous apheresis). *Atherosclerosis* 1987;68:19–25.
20. Yamamoto T, Yamashita T. Low-density lipoprotein apheresis using the Liposorber system: features of the system and clinical benefits. *Ther Apher* 1998;2:25–30.
21. Bambauer R, Schiel R, Latza R. Low-density lipoprotein apheresis: an overview. *Ther Apher Dial* 2003;7:382–90.
22. Tsurumi-Ikeya Y, Tamura K, Azuma K et al. Sustained inhibition of oxidized low-density lipoprotein is involved in the long-term therapeutic effects of apheresis in dialysis patients. *Arterioscler Thromb Vasc Biol* 2010;30:1058–65.
23. Nakamura T, Ushiyama C, Osada S, Inoue T, Shimada N, Koide H. Effect of low-density lipoprotein apheresis on plasma endothelin-1 levels in diabetic hemodialysis patients with arteriosclerosis obliterans. *J Diabetes Complications* 2003; 17:349–54.
24. Nakamura T, Kawagoe Y, Matsuda T et al. Effects of LDL apheresis and vitamin E-modified membrane on carotid atherosclerosis in hemodialyzed patients with arteriosclerosis obliterans. *Kidney Blood Press Res* 2003;26:185–91.
25. Kobayashi S, Oka M, Moriya H, Maesato K, Okamoto K, Ohtake T. LDL-apheresis reduces P-Selectin, CRP and fibrinogen—possible important implications for improving atherosclerosis. *Ther Apher Dial* 2006;10:219–23.
26. Morimoto S, Yano Y, Maki K, Sawada K, Iwasaka T. Efficacy of low-density lipoprotein apheresis in patients with peripheral arterial occlusive disease undergoing hemodialysis treatment. *Am J Nephrol* 2007;27:643–8.
27. Utsumi K, Kawabe M, Hirama A et al. Effects of selective LDL apheresis on plasma concentrations of ICAM-1, VCAM-1 and P-selectin in diabetic patients with arteriosclerosis obliterans and receiving maintenance hemodialysis. *Clin Chim Acta* 2007;377:198–200.
28. Hara T, Kiyomoto H, Hitomi H et al. Low-density lipoprotein apheresis for haemodialysis patients with peripheral arterial disease reduces reactive oxygen species production via suppression of NADPH oxidase gene expression in leucocytes. *Nephrol Dial Transplant* 2009;24:3818–25.
29. Tselmin S, Schmitz G, Julius U, Bornstein SR, Barthel A, Graessler J. Acute effects of lipid apheresis on human serum lipidome. *Atheroscler Suppl* 2009;10:27–33.
30. Duewell P, Kono H, Rayner KJ et al. NLRP3 inflammasomes are required for atherogenesis and activated by cholesterol crystals. *Nature* 2010;464:1357–61.
31. Rajamaki K, Lappalainen J, Oorni K et al. Cholesterol crystals activate the NLRP3 inflammasome in human macrophages: a novel link between cholesterol metabolism and inflammation. *PLoS ONE* 2010;5:e11765.
32. Kalousova M, Zima T, Tesar V, Sulkova S, Fialova L. Relationship between advanced glycoxidation end products, inflammatory markers/acute-phase reactants, and some autoantibodies

in chronic hemodialysis patients. *Kidney Int Suppl* 2003;63: S62–4.
33. Taki K, Takayama F, Tsuruta Y, Niwa T. Oxidative stress, advanced glycation end product, and coronary artery calcification in hemodialysis patients. *Kidney Int* 2006;70:218–24.
34. Mitsuhashi H, Tamura K, Yamauchi J et al. Effect of losartan on ambulatory short-term blood pressure variability and cardiovascular remodeling in hypertensive patients on hemodialysis. *Atherosclerosis* 2009;207:186–90.
35. Lee DM, Jackson KW, Knowlton N et al. Oxidative stress and inflammation in renal patients and healthy subjects. *PLoS ONE* 2011;6:e22360.
36. Stefanutti C, Di Giacomo S, Vivenzio A et al. Acute and long-term effects of low-density lipoprotein (LDL)-apheresis on oxidative damage to LDL and reducing capacity of erythrocytes in patients with severe familial hypercholesterolaemia. *Clin Sci (Lond)* 2001;100:191–8.
37. Stefanutti C, Vivenzio A, Ferraro PM, Morozzi C, Belotherkovsky D. Apheresis-inducible cytokine pattern change in severe, genetic dyslipidemias. *Cytokine* 2011;56:835–41.
38. Hovland A, Hardersen R, Sexton J, Mollnes TE, Lappegard KT. Different inflammatory responses induced by three LDL-lowering apheresis columns. *J Clin Apher* 2009;24:247–53.
39. Ehsan A, Mann MJ, Dell'Acqua G, Tamura K, Braun-Dullaeus R, Dzau VJ. Endothelial healing in vein grafts: proliferative burst unimpaired by genetic therapy of neointimal disease. *Circulation* 2002;105:1686–92.
40. Kizaki Y, Ueki Y, Yoshida K et al. Does the production of nitric oxide contribute to the early improvement after a single low-density lipoprotein apheresis in patients with peripheral arterial obstructive disease? *Blood Coagul Fibrinolysis* 1999; 10:341–9.
41. Sampietro T, Tuoni M, Ferdeghini M et al. Plasma cholesterol regulates soluble cell adhesion molecule expression in familial hypercholesterolemia. *Circulation* 1997;96:1381–5.
42. Tamai O, Matsuoka H, Itabe H, Wada Y, Kohno K, Imaizumi T. Single LDL apheresis improves endothelium-dependent vasodilatation in hypercholesterolemic humans. *Circulation* 1997;95:76–82.
43. Kone BC, Kuncewicz T, Zhang W, Yu ZY. Protein interactions with nitric oxide synthases: controlling the right time, the right place, and the right amount of nitric oxide. *Am J Physiol Renal Physiol* 2003;285:F178–90.
44. Yagi Y, Andoh A, Ogawa A et al. Microarray analysis of leukocytapheresis-induced changes in gene expression patterns of peripheral blood mononuclear cells in patients with ulcerative colitis. *Ther Apher Dial* 2007;11:331–6.

Hypertension
JOURNAL OF THE AMERICAN HEART ASSOCIATION

Enhanced Angiotensin Receptor-Associated Protein in Renal Tubule Suppresses Angiotensin-Dependent HypertensionNovelty and Significance

Hiromichi Wakui, Kouichi Tamura, Shin-ichiro Masuda, Yuko Tsurumi-Ikeya, Megumi Fujita, Akinobu Maeda, Masato Ohsawa, Kengo Azushima, Kazushi Uneda, Miyuki Matsuda, Kenichiro Kitamura, Shinichi Uchida, Yoshiyuki Toya, Hiroyuki Kobori, Kiyotaka Nagahama, Akio Yamashita and Satoshi Umemura

Hypertension. 2013;61:1203-1210; originally published online March 25, 2013;
doi: 10.1161/HYPERTENSIONAHA.111.00572
Hypertension is published by the American Heart Association, 7272 Greenville Avenue, Dallas, TX 75231

Print ISSN: 0194-911X. Online ISSN: 1524-4563